EFFECTS OF PPAR-GAMMA AGONIST ROSIGLITAZONE ON CARDIAC TISSUE AND CULTURED CARDIOMYOCYTES

By

DANA JOY DAVIS SCHREFFLER

A THESIS PRESENTED TO THE GRADUATE SCHOOL
OF THE UNIVERSITY OF FLORIDA IN PARTIAL FULFILLMENT
OF THE REQUIREMENTS FOR THE DEGREE OF
MASTER OF SCIENCE

UNIVERSITY OF FLORIDA

2013

To my family, and especially to my amazing husband, Jacob

ACKNOWLEDGMENTS

Through this long journey, many people have helped me, taught me and supported me. I would like to thank all of you from the bottom of my heart.

Special thanks go out to Dr. Wohlgemuth, who recognized my hard work and ambition and made it possible for me to pursue a graduate degree. Dr. Wohlgemuth has been a mentor and a friend and has always exhibited endless patience and support.

Thanks go to my committee members and undergraduate assistants who have helped me through my graduate endeavors: Dr. John Driver and Dr. Sally Johnson, Maria Guzman, Darah Kelley, Claire Kent and Yenny Ramirez-Lee. Each of my undergraduate assistants showed immense dedication through their long hours and hard work.

Thanks also go out to my family including my parents and amazing husband, Jacob, who has always provided me with unconditional love and everlasting support. None of this would have been possible without him. My mother and father have always been people I can count on, and without their love and support and help, I would not have successfully made it to the point I am in my life.

TABLE OF CONTENTS

page

LIST OF TABLES

LIST OF FIGURES

Abstract of Thesis Presented to the Graduate School
of the University of Florida in Partial Fulfillment of the
Requirements for the Degree of Master of Science

EFFECTS OF THE PPAR-GAMMA AGONIST ROSIGLITAZONE ON CARDIAC TISSUE AND CULTURED CELLS

By

Dana Joy Davis Schreffler

August 2013

Chair: Stephanie E. Wohlgemuth
Major: Animal Sciences

The peroxisome proliferator-activated receptor gamma (PPARγ) is a ligand-dependent transcription factor, responding to endogenous (i.e. fatty acids) and synthetic ligands. Thiazolidinediones are a family of synthetic ligands, including the anti-diabetic drug rosiglitazone. Through activation of PPARy, Thiazolidinediones increase storage of fatty acids, thereby increasing insulin sensitivity of hepatic tissue and skeletal muscle. This has led to treatment of Type II Diabetes mellitus with rosiglitazone (marketed as Avandia® by GlaxoSmithKline). However, adverse cardiovascular events in patients administered rosiglitazone have prompted the FDA to place the drug in a restricted access program.

We hypothesized that in rat heart and cultured adult human ventricular cardiomyocytes (AC16 cells) administration of rosiglitazone 1.) decreases mitochondrial function, and 2.) increases autophagy.

To test our hypotheses, Fischer 344 rats (5, 12 and 18 months old) received 10mg/kg/day rosiglitazone for 19 days; and AC16 cells were exposed to varying doses of rosiglitazone for 4 and 24 hours. We then determined mitochondrial enzyme activities

and mitochondrial respiration as measures of mitochondrial function, and expression of the autophagy protein LC3 to assess autophagy.

We found that rosiglitazone had no effect on mitochondrial enzyme activities, specifically cytochrome *c* oxidase and citrate synthase, in rat cardiac tissue and AC16 cells, and that the activity of these enzymes in rat heart was independent of age. Mitochondrial routine respiration and maximum electron transport capacity in AC16 cells were not affected by 10uM, but decreased by 200μM rosiglitazone. Autophagy was not affected by rosiglitazone, both *in vivo* and *in vitro.*

CHAPTER 1
INTRODUCTION

The peroxisome proliferator-activated receptors (PPARs) are a superfamily of nuclear hormone receptors, consisting of three isoforms: PPARα, which is prominently expressed in the liver; PPARβ/δ, which is most widely expressed in skeletal tissue; and PPARγ, which is expressed in white adipose tissue, the liver, and at moderate levels in the heart.

PPARs are ligand-dependent transcription factors with two types of ligands: endogenous ligands such as fatty acids, and exogenous, synthetic ligands, such as drugs in the Thiazolidinediones family (Spiegelman 1998). The ligand activates PPAR by binding to it. The activated PPAR associates with the Retinoid X Receptor (RXR), forming the PPAR response element (Berger *et al.* 2005), which drives the transcription of specific genes that will induce mechanisms such as differentiation of adipocyte, lipid storage, fatty acid oxidation, and insulin sensitization (Spiegelman 1998).

The Thiazolidinedione (TZD) family is a group of synthetic PPAR ligands (with greatest affinity for PPARγ), which includes the compounds pioglitazone, troglitazone, and rosiglitazone. The TZD's insulin-sensitizing effects led to its marketing as an anti-diabetic drug under the name Avandia® by the pharmaceutical company GlaxoSmithKline. Insulin resistance, a major contributor to Type 2 Diabetes mellitus (T2DM), has been linked to decreased mitochondrial oxidative activity and ATP synthesis, as well as high levels of circulating triglycerides in muscle and liver (Lowell and Shulman 2005). TZDs such as rosiglitazone increase lipid storage and fatty acid utilization, thus combating the insulin resistant condition of the Type 2 Diabetes mellitus patient. Despite its positive effects on insulin resistance, administration of Rosiglitazone

has been associated with a number of adverse effects, such as increased risk of myocardial infarction and cardiovascular mortality (Nissen & Wolski, 2010), and cardiac hypertrophy (Festuccia *et al.*, 2009). As a result, the FDA has restricted its use, and prescription of Rosiglitazone has become controversial in the United States (Pouwels & van Grootheest, 2012). It has therefore been of great interest to identify the underlying causes of rosiglitazone's negative effects on the heart. Recently, Rabol and colleagues (2010) evaluated the effects of Rosiglitazone on mitochondrial function in the skeletal muscle of patients with T2DM. The authors found that mitochondrial respiration was decreased in patients with T2DM compared to control subjects, an effect that was exacerbated by administration of rosiglitazone. It is, however, not known whether rosiglitazone has a negative effect on mitochondrial respiration in the heart as well. In this study we hypothesized that administration of rosiglitazone decreases mitochondrial function in the heart. To test out hypothesis we investigated the effect of rosiglitazone on mitochondrial function in heart tissue from rats that had been administered rosiglitazone, and in a cultured cardiomyocyte cell line.

In addition to its effects on mitochondrial metabolism, few *in vitro* studies have investigated the effect of PPARγ activation on the cellular quality control mechanism autophagy. Autophagy is a cellular housekeeping mechanism by which cells typically sequester portions of cytoplasm, which can include organelles, protein aggregates and cellular waste, into autophagosomes and deliver these to lysosomes for degradation. Besides its role as housekeeping mechanism, this process is activated in conditions of energy imbalance and serves to supply substrates for energy production.

The reports on the effect of PPARγ activation on autophagy have been conflicting. While PPARγ activation has been shown to induce autophagy in breast cancer cells (Zhou *et al.* 2009) and adrenocortical cancer cells (Cerquetti *et al.* 2011), Mahmood *et al.* (2011) reports that PPARγ inhibits autophagy and induces apoptosis in human monocyte-derived macrophages, but there have been no reports on the effect of PPARγ on autophagy in the heart. Both too much and too little autophagy can be detrimental to an organ system, making this a necessary niche to explore (Troncoso *et al.* 2013). In this study, we hypothesize that administration of rosiglitazone increases autophagy in the heart, leading to a reduction in heart remodeling and contributing to the likelihood of cardiovascular mortality. To test this hypothesis, we examined the effect of rosiglitazone on autophagy and on autophagic flux in heart tissue from rosiglitazone-treated rats and in cultured cardiomyocytes.

The objectives of the current study were (1) to assess the effect of rosiglitazone on mitochondrial function and content in the heart, (2) to determine if this effect is age-dependent, and (3) to determine if rosiglitazone has an effect on autophagy in the heart.

CHAPTER 2
MATERIALS AND METHODS

Experimental Subjects and Design

In vivo Experiments

Animals

Fischer 344 rats were purchased from the National Institute of Aging (NIA) colony at Harlan Laboratories (Indianapolis, IN). The experimental groups consisted of rats of three ages: 5 months (n=19), reflecting a young age; 12 months (n=21), reflecting adulthood; and 18 months (n=21), reflecting onset of senescence. Rats were received and housed for 1 week prior onset of the experimental treatment. Rats were individually housed and maintained on a 12-h light/dark cycle under controlled conditions. Health status, body weight and food intake were monitored daily. The rats had free access to regular rat chow, and to tap water. Principles of laboratory animal care (NIH publication No. 86-23, revised 1985) were followed and all procedures were approved by the University of Florida's animal care and use committee.

Experimental Treatment

Seven days after arrival, the experimental treatments and assessments were started. All rats were given plain frozen strawberry milk treats starting two days prior to water maze training, and vehicle treats (2.5% ethanol/strawberry milk, v/v) throughout training and testing to familiarize the rats with the treat and administration paradigm. Based on water maze performance (used for a concurrent study), rats of each age were randomly assigned to the experimental groups: the treatment group, which received rosiglitazone (5 months, n = 11; 12 months, n = 10; and 18 months, n = 10), or the control group, which received vehicle (5 months, n =9; 12 months, n = 11; and 18

months**,** n = 11). After completing the initial water maze training and testing, the experimental drug exposure was started in which rats were either given 500 μL frozen strawberry milk treats containing rosiglitazone (5 mg/kg; Cayman Chemical Company, Ann Arbor, MI, USA), or containing vehicle (2.5% ethanol v/v) twice daily for 19 days. Rats were all euthanized in the morning.

Before euthanization, rats were weighed, subsequently sedated using isofluorane, and then euthanized with a guillotine. Following decapitation, the chest was opened and the heart excised. The heart was immediately flushed with saline, blotted dry, weighed, and then flash-frozen in liquid nitrogen. The tissues were stored in liquid nitrogen until time of use. All rats in this study were treated in accordance with the policies set forth by the University of Florida Institutional Animal Care and Use Committee (IACUC) and the National Institutes of Health (NIH) regarding the ethical use of animals for experimentation.

In vitro **Experiments**

Cells

The *in vivo* study was complemented with *in vitro* experiments using an immortalized cardiac cell line, reflecting as closely as possible the heart tissue examined in the *in vivo* experiments. Using cultured cells had the advantage that the effects of different concentrations of rosiglitazone and durations of rosiglitazone exposure could be evaluated. AC-16 human derived ventricular cardiomyocytes (Garbern *et al.* 2013) were generously donated by Dr. Leeuwenburgh, UF, and used to evaluate the effect of rosiglitazone on 1) mitochondrial function using High Resolution Respirometry (HRR), 2) mitochondrial enzyme activity via spectrophotometric enzyme activity assays, and 3) expression of autophagy-regulatory proteins using Western

Blotting. The cells were maintained in Dulbecco's Modified Earle's Medium F-12 50/50 containing 10% FBS, 29mM sodium bicarbonate, 2.5mM glutamine, 17.5mM glucose, 1.25mM sodium pyruvate, and 50IU penicillin mixed with 50uM streptomycin at pH 7.2 in an incubator at 37°C with 5%$CO_{2.}$

Experimental Treatment

Rosiglitazone treatment: For a rosiglitazone exposure experiment, cells were seeded into 6-well plates (Corning) in normal growth medium and grown to 90% confluency, which amounted to approximately 0.5 x 10^6 cells. Prior to the experimental treatment, each well was washed once with PBS. Cells were then exposed to growth medium containing vehicle (0.1% DMSO) or 10, 100 or 200 µM rosiglitazone dissolved in DMSO (purchased from Cayman Chemicals) for 4 or 24 hours. In order to limit the cells' exposure to DMSO, a 100 mM rosiglitazone stock solution was prepared, aliquoted and stored at -20 °C, and heated to 72 °C prior to use. At the beginning of the experiment, an appropriate amount of rosiglitazone stock solution was added to the respective medium, ensuring a final DMSO content of ≤ 0.1% DMSO. At the end of the exposure the cells were either lysed and the cell lysates frozen at -80 °C until performance of biochemical analyses (enzyme activity assays; Western Blot; see below), or trypsinized, washed in normal culture media and injected into the respirometer chamber for determination of cellular respiration by High Resolution Respirometry (see below). Experimental replicates were performed on different days using a different cell passage. Each experiment included control cells, which were maintained in normal growth medium and exposed for the same amount of time than the simultaneously rosiglitazone-treated cells.

Measurement of autophagy and autophagic flux

Control cells were maintained in normal growth medium without rosiglitazone, with vehicle (0.1% DMSO). The autophagic flux was quantified by adding Bafilomycin A1 (50nM final concentration) to a duplicate well of each treatment. Bafilomycin A1, a proton pump inhibitor, which prevents the fusion of the autophagosome with the lysosome by neutralizing the lysosomal pH, causes the accumulation of autophagosomes (Rubinsztein *et al.* 2009). Because the final degradation of the autophagosomes and their contents is prevented, the autophagosomal membrane-bound form of the autophagy marker protein LC3-II accumulates. LC3-II accumulation can then be utilized to determine the autophagic flux by calculating the difference of LC3-II protein level between the cells treated without and the cells treated with Bafilomycin A1 within the same treatment (Rubinsztein *et al.* 2009). Two independent experiments were performed to determine the effect of rosiglitazone on autophagic flux in AC-16 cells.

Cells for measurement of cellular respiration

Cells used for determination of cellular respiration in the absence and presence of rosiglitazone were maintained in T-25 flasks. Per experiment two flasks were prepared and cells grown to 90% confluency. For the experiment, the cells in one flask were maintained in normal growth medium (control), and the cells in the other flask were exposed to growth medium containing rosiglitazone (treatment; 10, 100, or 200 μM final concentration; see above). At the beginning of the experimental exposure, the normal growth medium was exchanged for either control medium or treatment medium. At the end of the experimental exposure, the medium was removed, cells were washed once with PBS, subsequently trypsinized and a cell count performed. Cells were added

to each of the two respirometer chambers in a final concentration of 0.3 – 0.5 x 10^6 mL^{-1} cells. Each respirometer assessment was performed on control and rosiglitazone-treated cells side by side. Cellular respiration was measured in five treatments groups: Control (n=20), 10 μM rosiglitazone for 4 hours (n=4), 200 μM rosiglitazone for 4 hours (n=5), 10 μM rosiglitazone for 24 hours (n=5), and 200 μM rosiglitazone for 24 hours (n=4). (for more details see "High Resolution Respirometry" below)

Processing of Cardiac Tissue

Heart Size

Heart weight was determined and then normalized to body weight. Normalized heart weight was analyzed across treatments and ages.

Preparation of Cardiac Tissue for Different Analyses

Homogenization of cardiac tissue for spectrophotometric enzyme activities

The rat hearts, collected and stored in liquid nitrogen as described above, were homogenized using a liquid nitrogen-cooled Biopulverizer (BioSpec products, Bartlesville, OK). The powdered tissue (15-20mg) was transferred to a liquid nitrogen-cooled microcentrifuge tube, and 50 μL of extraction buffer (0.1M KH_2PO_4 buffer with 2mM EDTA; pH 7.2; Adhihetty *et al.*) added. The tissue suspension was mixed by tapping and then further diluted 20-fold (w/v) with extraction buffer. Following incubation and shaking on a thermomixer (Eppendorf, Hamburg, Germany) at room temperature for 15 minutes at 1400 rpm, the samples were sonicated on ice using a sonic dismembrator (Fisher) at a setting of 7 (on a scale of 1 to 20) for 3 x 3 seconds. The samples were then again diluted with extraction buffer to a final 80-fold dilution. The final tissue extracts were centrifuged at 14,000 x *g* for 2 minutes at room temperature.

The supernatant was transferred to a new tube and the protein concentration determined using the Bradford assay (Fisher).

Homogenization of cardiac tissue for immunoblot

For immunobloting, the cryo-pulverized heart tissue (see above) was suspended in 10µL/mg tissue in homogenization buffer containing 250mM Sucrose (Sigma), 1mM EDTA (Fisher), 2% SDS (Sigma), 10mM TRIS base (Fisher Scientific), and 1% Protease Inhibitor Cocktail (ThermoScientific); pH 8. The samples were vortexed for 15 seconds, and heated at 95 °C 3 x 3 minutes with 15 seconds of vortexing in between. The samples were then centrifuged for 10 minutes at 12,000 x *g* at room temperature, transferred to a new tube and the protein concentration determined using the Bradford assay (Fisher).

Processing of AC16 Cells

Homogenization of AC16 Cells for Spectrophotometric Enzyme Activities

AC16 cells were seeded to confluency in a 6-well plate and treated for 4 hours with 0 (vehicle only), 10uM, 100uM or 200uM rosiglitazone as described above. After the four hour exposure to rosiglitazone or vehicle, the experimental media was removed, and the cells quickly washed with ice-cold PBS (Phosphate Buffered Saline, Lonza, Walkersville, MD). Subsequently, 100 µl of cell preparation buffer (0.25 M sucrose, 40mM potassium chloride, 2 mM EGTA, 1 mg/ml bovine serum albumin, and 20 mM Tris-HCl; pH 7.2; Campian *et al.* 2007) was added to each well followed by rotating the plate at 4 °C for 5 minutes. The cells were scraped off and transferred into a microcentrifuge tube. The cell suspensions were then rotated at 4 °C for 30 minutes. Afterwards, the cells were lysed by sonicating on ice using a sonic dismembrator (Fisher Scientific) at setting 3 (on a scale of 1 to 20) for 10 one second

bursts. The cell lysates were then centrifuged at 2000 x *g* for 10 minutes at 4 °C, and the supernatant transferred to a new tube. Prior to enzymatic activity assays, the protein concentration in the lysates was determined using the Bradford assay (Fisher Scientific) according to the manufacturer's instructions. Cell lysates were stored at -80°C until enzyme assays (see below).

Homogenization of AC16 Cells for Immunoblot

AC16 cells were seeded to confluency in a 6-well plate and treated for four hours with 0 (vehicle only), 10uM, 100uM or 200uM rosiglitazone, with or without bafilomycin A1 (25 nM final concentration). At the end of the exposure, the experimental media was removed, and each well rinsed with ice-cold PBS buffer, as described above. Then, 100uL of ice-cold RIPA lysis buffer (ThermoScientific, Rockford, IL), containing 1mM PMSF (Sigma, St. Louis, MO), and 1% Protease inhibitor cocktail (ThermoScientific, Rockford, IL) was added to each well. The plates were then rotated at 4 °C for 5 minutes. The cell lysates were scraped off and transferred into individual microcentrifuge tubes and rotated at 4 °C for 30 minutes. Cell lysates were the sonicated on ice with a sonic dismembrator for 10 one second bursts at a setting of 7 (on a scale of 1 to 20). After sonication, the samples were centrifuged at 14000 x *g* at 4°C for 10 minutes, and the supernatant transferred to new tubes. Protein concentration was determined using the BCA assay (ThermoScientific) according to the manufacturer's instructions. Samples were aliquoted and stored at -80 °C until further analysis.

Mitochondrial Function Measurements

Cytochrome *c* Oxidase Activity

Cytochrome *c* Oxidase (COX) activity in AC16 cell lysates was determined with a spectrophotometric enzyme activity assay modified after Smith (1955). Briefly, a solution of reduced horse heart cytochrome *c* (cyt *c*; 2 mg/mL; Sigma, St. Lous, MO), serving as substrate for COX, was prepared in 100 mM KPO4 buffer (pH 7.0) using 57 mM sodium dithionite (in 10 mM KPO4) as a reducing agent. Enzyme activity was determined from the rate of oxidation of reduced cyt *c* at 30 °C, measured as reduction in absorbance at 550 nm using a microplate reader (Synergy HT, Biotek Instruments, Winooski, VT; Gen5 operating software). COX activity is reported in µmol/min/mg protein. See Appendix I for detailed protocol.

Citrate Synthase Activity

The activity of Citrate Synthase (CS) in AC16 cell lysates was determined with a spectrophotometric enzyme activity assay as described in Kuznetsov *et al.*. (2010). In this assay, the production of Coenzyme A by CS from Oxaloacetate and Acetyl CoA is coupled to the irreversible reaction of Coenzyme A with DTNB (5,5-dithiobis-2-nitrobezoate), producing TNB (thionitrobenzoic acid). The absorbance of TNB is measured at a wavelength of 412 nm using a microplate reader. The reaction mix contained a final concentration of 0.25% Triton X-100, 0.31 mM Acetyl CoA (30 mM stock in water), 0.1 mM DTNB (1.01 mM stock in 1.0 M Tris-HCl buffer, pH 8.1), and 8 µg of protein from muscle homogenate or cell lysate. The reaction was started by addition of 0.5 mM Oxaloactetate (10 mM stock in 0.1 M triethanolamine, pH 8.0). Citrate Synthase activity is reported in µmol/min/mg protein. See Appendix II for detailed protocol.

High Resolution Respirometry

Oxygen consumption of intact AC 16 cells was measured as an indicator of mitochondrial function using a high resolution respirometer (Oroboros O2K Oxygraph, Innsbruck, Austria). In brief, a polarographic oxygen sensor detects the oxygen concentration inside a closed respirometer chamber, which contains the cells. The data output is reported as oxygen concentration over the course of time and as its first derivative, which is the oxygen consumption rate, or oxygen flux. After an experimental treatment, cells were trypsinized and counted, and 300,000-500,000 cells/mL added to each of the two 2-mL chambers of the oxygraph. Oxygen consumption was measured in the two chambers simultaneously, such that oxygen flux of control and Rosiglitazone-treated cells were assessed side by side. The inhibitors oligomycin (2ug/ml), rotenone (final concentration 0.5 μM), and antimycin A (final concentration 2.5 μM), and the uncoupler FCCP (carbonyl cyanide 4-(trifluoromethoxy) phenylhydrazone; in 0.5 μM steps up to a maximum final concentration of 3 μM), were titrated into the closed respirometer chamber in a specific sequence: 1. Oxygen flux of intact cells in culture media (Routine respiration; physiologically coupled respiration in the intact cell); 2. Addition of the ATP-synthase inhibitor oligomycin (LEAK state; respiration compensating for the proton leak, proton slip, and cation cycling); 3. Addition of FCCP (uncoupled respiration, or excess capacity; respiration in the presence of a protonophore (i.e. FCCP) which cycles across the inner mitochondrial membrane with transport of protons and dissipation of the electrochemical proton gradient); 4. Addition of the Complex-I inhibitor rotenone (respiration with Complex-II substrates only); and 5. Addition of the Complex-III inhibitor antimycin A (residual, non-mitochondrial, oxygen consumption). The residual oxygen consumption is subtracted as extra-mitochondrial

from the mitochondrial oxygen consumption. Oxygen consumption rate, or oxygen flux, is reported in pmol O_2 s^{-1} (10^{-6} cells. Based on these recorded oxygen flux measures the following respiratory control ratios were calculated: Routine Control Ratio (Routine/ETS), a ratio expressing how close routine respiration operates to ETS capacity, and LEAK Control Ratio (LEAK/ETS), which is the ratio between respiration in the presence of the ATP-synthase inhibitor oligomycin, and maximal electron transport system capacity (ETS).

Western blot analysis

Expression of LC3 B, an integral autophagy-regulating protein, and GAPDH, glyceraldehyde 3-phosphate dehydrogenase, a housekeeping protein, in cardiac tissue and AC16 cells was determined using western blot analysis of tissue extracts and cell lysates, respectively. Cardiac tissue homogenates and AC16 cells were homogenized and lysed respectively, as described above, and the tissue extracts and cell lysates prepared for SDS-PAGE electrophoresis followed by Western Blot. Prior to loading on a denaturing SDS polyacrylamide gel, extracts and lysates were mixed 1:2 with Laemmli buffer (62.5 mM Tris–HCl, 2% SDS, 25% Glycerol, 0.01% Bromophenol Blue, pH 6.8; BioRad, Hercules, CA) containing the reducing agent β-mercaptoethanol, and boiled at 95 °C for 10 minutes. Equal amounts of protein (50 µg cardiac tissue extract; 20 µg cell lysate) were applied to pre-cast Tris-HCl gels (Criterion system, BioRad) formulated as “any kDa” acrylamide (proprietary formulation). Gels were run at 200V for approximately 50 minutes using Tris-Glycine-SDS running buffer (BioRad). After electrophoretic separation, the proteins were transferred to polyvi polyvinylidene difluoride (PVDF) membrane (Immobilon P, 0.45 lm, Millipore, Billerica, MA) using a semidry blotter (BioRad) at a constant 7V for 2.5 hours. The transfer buffer (Tris-Glycine; BioRad)

contained 15% methanol. After the transfer, the membranes were rinsed in dH_2O and methanol, and let dry for at least 15 min to optimize protein binding to the membrane. Transfer efficiency and quality was subsequently verified by staining the membrane with Ponceau S (Sigma-Aldrich). Membranes were then blocked in Tris-buffered saline (137mM NaCL, 2.7mM KCl, and 24.76mM Tris Base) with 0,05% Tween-20 (Fisher) (TBS-t) containing 5 % (w/v) non-fat dry milk (Blotting-Grade Blocker, BioRad, Hercules, CA) for one hour at room temperature; subsequently washed in TBS (without Tween), and incubated overnight in the corresponding primary antibody (see below) at 4 °C. Subsequently, membranes were washed in TBS-t and incubated with horseradish perioxidase (HRP) conjugated secondary antibody (Sigma-Aldrich) at room temperature for one hour. Membranes were then washed in TBS-t, followed by TBS. Finally, the DuoLux chemiluminescent/fluorescent substrate for HRP (Vector Laboratories, Burlingame, CA) was applied for 5 min, followed by a quick rinse with Tris–HCl (100 mM, pH 9.5), and the chemiluminescent signal captured with a Syngene G-BOX imager (Synoptics Group, Frederick, MD).The digital images were analyzed using SynGene software (Synoptics Group, Frederick, MD). Density of the target band was normalized to GAPDH (Glyceraldehyde 3-phosphate dehydrogenase), and expressed in arbitrary optical density units.

Antibodies used were LC3B (1:1000, Cell Signaling, Danvers, MA), GAPDH (1:1000, Cell Signalling), and HRP-linked secondary antibodies (1:50,000, Sigma). Add clone names

Statistical Analysis

For both heart tissue and cultured cells, the experiments were fully crossed, two-factor designs with two or three levels for each factor: a) heart: 1) age (5, 12 and 18

months) and rosiglitazone (vehicle without rosiglitazone, “control”, and vehicle with rosiglitazone, “treatment”); and b) cultured cells: exposure time (4 and 24 hours) and rosiglitazone (0, 10, 100, 200 μM). The Two-Way analysis of variance (ANOVA) will allow us to distinguish between the effects of age (*in vivo* study) or exposure time (*in vitro* study), respectively, and the presence of the drug rosiglitazone, and a possible interaction effect between age/exposure time and drug. *Post hoc* multiple comparisons for all ANOVA tests were performed with the Tukey HSD procedure. A Kruskal-Wallis ANOVA on Ranks test was performed when data were not normally distributed.
Enzyme activities in AC16 cells were compared between experimental groups in a One-Way ANOVA, with dose of rosiglitazone as the independent factor (only one exposure time was tested). Heart size normalized to body weight and enzyme activities in heart tissue extracts were analyzed using a Two-Way ANOVA with age and dose of rosiglitazone as independent factors. Protein expression data were analyzed using a One-Way ANOVA (AC16 cells) or a Two-Way ANOVA (heart), respectively.
All statistical analyses were conducted using SigmaPlot vs. 12 (Systat Software, Inc., San Jose, CA), with $p \leq 0.05$ accepted as significant.

CHAPTER 3
LITERATURE REVIEW

A constant supply of energy is essential for maintenance of heart activity. The heart's energy demand is met primarily by β-oxidation of fatty acids, which support 60-90% of cardiac energy supply, and subsequent oxidation of reduction equivalents in the mitochondrial oxidative phosphorylation (OXPHOS) system. The heart relies heavily on oxidative phosphorylation for energy production, which accounts for over 90% of the ATP produced, and there is a complex interplay of receptors and co-factors that must be engaged to activate energy production pathways in order meet these demands (Kodde et al. 2006). The nuclear hormone receptor family of peroxisome proliferator-activated receptors (PPARs) is an intrinsic part of the regulatory system to ensure energy balance in the heart.

Peroxisome Proliferator-Activated Receptors (PPARs) and Their Physiological Effects

The members of the PPAR family are transcription factors that are major regulators of energy homeostasis and metabolic functions (Tyagi *et al.* 2011). The PPAR receptor family consists of 3 receptor subtypes: 1) PPARα, which is prominently expressed in the liver, where it plays a major role in fatty acid oxidation and lipid metabolism; 2) PPARβ/δ, which is most widely found in skeletal muscle tissue, where it acts as a metabolic sensor and fatty acid regulator, and 3) PPARγ, which is expressed in white adipose tissue, the liver, and at moderate levels in the heart, regulates adipocyte differentiation, fatty acid storage and glucose metabolism (Edvardsson *et al.* 1999; Ehrenborg & Krook, 2009). All three PPAR subtypes function as lipid sensors, which, when activated, will associate with a retinoid X receptor (RXR). The heterodimer will translocate into the nucleus and bind to a specific DNA sequence, the peroxisome

proliferator response element (PPRE). The association of the heterodimer with the PPRE activates transcription of specific genes involved in the metabolic functions outlined above. The PPARs are activated by small lipophilic ligands such as fatty acids, which occur endogenously, and synthetic drugs such as compounds in the insulin sensitizing Thiazolidinedione (TZD) family (Tyagi *et al.* 2011).

Their role in regulation of metabolic functions and the well-defined therapeutic actions of their synthetic ligands make PPARs ideal targets for metabolic disease intervention. For example, due to the role of PPARα in lipid metabolism, its (synthetic) agonists are employed as anti-atherosclerotic and hypolipidemia agents, to combat dyslipidemia associated with metabolic syndrome (Berger *et al.* 2005; Tyagi *et al.* 2011). Obesity and inflammation have also been treated with PPAR agonists. Activation of PPARα by therapeutic synthetic ligands has been shown to attenuate obesity in rodents by increasing hepatic fatty acid oxidation and decreasing the levels of triglycerides responsible for adipose tissue hypertrophy, while PPARγ agonists have been demonstrated to inhibit the expression of inflammatory cytokines (Tyagi *et al.* 2011). Currently, PPARγ agonists are largely used as a therapeutic approach to treat insulin resistance.

Their role in regulation of metabolic functions and the well-defined therapeutic actions of their synthetic ligands make PPARs ideal targets for metabolic disease intervention. For example, due to the role of PPARα in lipid metabolism, its (synthetic) agonists are employed as anti-atherosclerotic and hypolipidemia agents, to combat dyslipidemia associated with metabolic syndrome (Berger *et al.* 2005; Tyagi *et al.* 2011). Obesity and inflammation have also been treated with PPAR agonists. Activation of

PPARα has been shown to attenuate obesity in rodents by increasing hepatic fatty acid oxidation and decreasing the levels of triglycerides responsible for adipose hypertrophy, while PPARγ agonists have been demonstrated to inhibit the expression of inflammatory cytokines (Tyagi *et al.* 2011). Currently, PPARγ agonists are largely used as a therapeutic approach to insulin resistance.

Peroxisome Proliferator-Activated Receptor Gamma (PPARγ)

PPARγ is predominantly expressed in adipose tissue where it is expressed 10- to 30-fold higher than in other tissues, such as the liver and cardiac tissue (Spiegelman 1998). PPARγ is known to function as a master regulator for adipocyte differentiation as well as regulating fatty acid storage and glucose metabolism (Tyagi *et al.* 2011). Agonists of PPARγ are widely used as insulin sensitizing drugs. In adipose tissue, PPARγ ligands exert an insulin sensitizing effect by altering the expression of genes that are involved in lipid uptake, lipid metabolism and insulin action, thereby enhancing adipocyte insulin signaling, lipid uptake and anabolic lipid metabolism and attenuating free fatty acid release. In hepatic and surrounding tissues, PPARγ activation lowers the levels of circulating free fatty acids. By lowering the fat content of the pancreatic islet β-cells, excessive apoptosis is inhibited and the β-cell population is sustained, thus allowing for more efficient glucose clearance (Berger *et al.* 2005). In addition to reducing insulin resistance by modifying lipid metabolism, activation of PPARγ by TZD's has been demonstrated to cause an accumulation of small adipocytes while promoting apoptosis in large, mature adipocytes. This shift in adipocyte population favors insulin sensitivity, as the small adipocytes are intrinsically more insulin sensitive than large adipocytes (Zieleniak *et al.* 2008). Thus making PPARγ agonists ideal targets for the treatment of Type II diabetes mellitus (T2DM).

T2DM is a metabolic syndrome primarily associated with decreased insulin sensitivity of tissues, generally stemming from defects in the secretion of insulin by pancreatic β cells (Lowell & Shulman, 2005) Lifestyle choices, such as poor diet and lack of exercise, combined with genetic predisposition for diabetes are major risk factors for the onset of T2DM (Riserus *et al.* 2009).

Thiazolidinediones (TZDs) are synthetic ligands that bind to PPARγ with high affinity, without binding to the other PPAR subtypes (α, β/δ). Members of the class of TZDs, derivatives of the thiazolidinedione, include the compounds troglitazone, pioglitazone, and rosiglitazone. Pharmacological administration of TZDs were approved for treatment of T2DM by the FDA starting with troglitazone in 1996, manufactured under the names Rezulin® or Romozin®. Troglitazone has since been removed from the market in the US due to its hepatotoxic side effects (Koffarnus *et al.* 2013; Yau *et al.* 2013). Pioglitazone is currently marketed under the name Actos® by Takeda and approved for prescription to treat T2DM, and rosiglitazone is currently marketed under the name Avandia by GlaxoSmithKline. Rosiglitazone has been removed from market in Europe and New Zealand, and the FDA has restricted its use in the US due to the increased risk of adverse cardiovascular effects such as myocardial infarction and cardiac death (Koffarnus *et al.* 2013; Nissen & Wolski, 2007).

PPARγ-Dependent Effects of TZDs

Insulin sensitizing effect. Insulin resistance has been linked to decreased mitochondrial oxidative activity and ATP synthesis, as well as high levels of circulating triglycerides in muscle and liver (Lowell & Shulman, 2005). Oxidative phosphorylation of fatty acids is normally responsible for about 60-90% of the ATP synthesis in the human heart (Stanley *et al.* 1997) . In the diabetic patient, both glucose and lactate uptake is

impaired, leading to an even greater reliance on oxidative phosphorylation of free fatty acids (Stanley *et al.* 1997). At the same time, oxidation of fatty acids is impaired, leading to higher levels of circulating free fatty acids. It is thought that these high levels of circulating free fatty acids compete with two enzymes required for glucose utilization, pyruvate dehydrogenase and phosphofructokinase, causing inhibition of the glycolytic pathway, and thus increasing insulin resistance (Lowell & Shulman, 2005).

Due to their insulin sensitizing effects, TZD's are widely prescribed for the treatment of T2DM. These compounds are known for directly activating PPARγ, which regulates fatty acid storage and utilization and glucose homeostasis (Koffarnus *et al.* 2013). In experiments studying the efficacy of TZDs, it was determined that these compounds improve glucose tolerance and insulin resistance by increasing insulin sensitivity of hepatic tissue and muscles and preserving β cell function (Yau *et al.* 2013; Fryer *et al.* 2002).

Receptor-Independent Effects of TZDs

In addition to its receptor-dependent actions, such as fatty acid storage and use, insulin sensitizing effects and anti-inflammatory effects, TZDs have been shown to exert receptor-independent actions (Feinstein *et al.* 2005). These effects, which are independent of direct effects on gene transcription, may be the underlying cause for some of the effects that are not metabolism related. For example, TZD's have been shown to activate the adenosine monophosphate-activated protein kinase (AMPK) pathway, inhibit inflammatory cytokines, suppress cell proliferation and disrupt mitochondrial function (Feinstein *et al.* 2005; Bolten *et al.* 2007).

Bolten and colleagues (2007) and Brunmair and colleagues (2001) suggested that TZDs activate the AMPK pathway. AMPK is a master regulator of energy metabolism. It

is activated by an increase in the intracellular AMP/ATP ratio, and considered a sensor for cellular energy imbalance (Feinstein *et al.* 2005; Dyck & Lopaschuk, 2006). In a 2002 study by Fryer and colleagues, it was demonstrated that TZD's, specifically rosiglitazone, directly activate the AMPK pathway in skeletal muscle, which lead to the inhibition of mitochondrial OXPHOS. In the same journal article, it was stated that long term activation of AMPK has been shown to increase the expression of a number of proteins that lead to an increase in insulin sensitivity. These overlapping effects, both metabolic effects and insulin sensitizing effects, of AMPK and TZD's makes it difficult to determine if TZD's are causing mitochondrial dysfunction and thus stimulating AMPK due to the subsequent energy imbalance or if it is a direct effect of TZD's on AMPK. Feinstein and colleagues (2005) speculate that activation of AMPK may be dependent upon TZD induced changes in metabolic state and mitochondrial impairment.

Mitochondrial Function

Mitochondria are intracellular double-membrane enclosed organelles that generate most of the cell's ATP. Under physiological conditions, a series of enzyme complexes and electron carriers (collectively termed electron transport chain or system) located at the inner mitochondrial membrane transfer electrons from the reduction equivalents NADH and $FADH_2$, produced in glycolysis and the citric acid cycle, to the ultimate electron acceptor oxygen, thereby producing H_2O. Enzyme complex I, II and IV of the electron transport system (ETS) utilize the energy released by this electron transfer to pump protons from the mitochondrial matrix into the intermembrane space (IMS), thereby creating an electrochemical gradient across the inner mitochondrial membrane. This electrochemical gradient is utilized to produce ATP from ADP and inorganic phosphate, and is catalyzed by the inner mitochondrial membrane enzyme

ATP synthase, which allows the exergonic transport of protons back into the matrix. The process of electron transport coupled with ADP phosphorylation is commonly referred to as oxidative phosphorylation (Spinazzi *et al.* 2012;Gnaiger 2012).

There are several methods to assess mitochondrial function. The most common approach is to determine mitochondrial oxygen consumption or respiration. This approach takes advantage of the fact that oxygen is the terminal electron acceptor in the mitochondrial ETS, The rate of oxygen consumption in a closed (air-tight) chamber containing living cells (or biological material such as tissue or isolated mitochondria) can therefore be used as an indicator of mitochondrial electron transport function (Spinazzi *et al.* 2012). Depending on the biological material assessed (tissue, intact cells, permeabilized cells, isolated mitochondria), a series of different energy substrates, inhibitors of mitochondrial respiratory enzyme complexes, and mobile ion carrier (also called uncoupler of oxidative phosphorylation) are sequentially titrated into the measuring chamber and subsequent oxygen consumption recorded

There are four major states of mitochondrial respiration used to assess their overall function. Routine respiration measures respiration of the cell sample in an unaltered state, prior to offering substrates or ADP. LEAK respiration is measured after inhibition of the ATP synthase and accounts for any mitochondrial respiration not linked to the phosphorylation system, such as proton leaks or slips, cation cycling, and ROS production (Gnaiger 2012). ETS is defined as excess, or maximum, capacity of the electron transport system, and is measured in the presence of an uncoupler, such as FCCP (Carbonyl cyanide-4-(trifluoromethoxy)phenylhydrazone)**.** By uncoupling proton flow from electron transfer, true maximum capacity can be assessed demonstrating full

electron transfer efficiency. Finally, residual oxygen consumption (ROX) is assessed in the presence of antimycin A, a complex III inhibitor. When antimycin A is introduced, it effectually shuts down the electron transport system allowing the contribution to respiration by the cell to be accounted for.

These respiratory states can then be compared in ratio form to assess other important parameters of mitochondrial function such as coupling efficiency (LEAK/ETS), and the routine control ratio (Routine/ETS). Assessing LEAK/ETS determines how "coupled" oxygen consumption is to the phosphorylation system. Routine/ETS demonstrates to what extent routine is contributing to the overall capacity of the electron transport system.

Another method to evaluate mitochondrial function is to determine enzymatic activity of mitochondrial enzymes using a spectrophotometric enzyme assay (see materials and methods section). Most commonly, complex IV of the ETS, or cytochrome *c* oxidase, and citrate synthase, an enzyme of the citric acid cycle located in the mitochondrial matrix, are used as markers of mitochondrial function. Moreover, activity of citrate synthase has been shown to correlate well with mitochondrial content and has therefore been used as a marker for this parameter (Campian *et al.* 2007;Chrzanowska-Lightowlers *et al.* 1993).

Autophagy

AMPK will employ autophagy when the AMP:ATP ratio is high. This will lead to a signaling cascade that will culminate in the degradation of aggregate proteins, thereby restoring the supply of amino acids for energy production (Vacek *et al.* 2011). Autophagy is cellular housekeeping mechanism by which cellular constituents, such as proteins, protein aggregates, and cell organelles, are sequestered within a double-

membrane bound organelle, the autophagosome, which subsequently fuses with a lysosome, which delivers the enzymes for the degradation of the sequestered cellular material (Cuervo 2008; Rubinsztein *et al.* 2009). Autophagy is thereby a catabolic process that serves the degradation and recycling of cellular constituents. It is a highly regulated process, and a variety of stimuli can initiate this process, such as the disruption of mitochondrial membrane potential, nutrient deficiency, and pharmacological agents such as rapamycin (Cuervo 2008; Cerquetti *et al.* 2011). One of the major regulatory pathway regulators at which some of the inducers and inhibitors of autophagy merge for autophagy is mTOR, the mammalian target of rapamycin (Vacek *et al.* 2011). AMPK is an example of a kinase that merges at the mTOR complex to induce autophagy.

Both, too much autophagy and too little autophagy can be detrimental to an organ system. Deregulation of autophagy has been implicated in a number of pathologies such as cardiovascular disease, diabetes and cancer (Troncoso *et al.* 2013). Little research has been reported on the effects of PPARγ stimulation, via TZD's or otherwise, on autophagy, with the findings being cell-specific results. For example, PPARγ has been shown to induce autophagy in breast cancer cells (Zhou *et al.* 2009) and adrenocortical cancer cells (Cerquetti *et al.* 2011), while Mahmood *et al.* (2011) reports that PPARγ inhibits autophagy and induces apoptosis in human monocyte-derived macrophages, but there are no reports on the effects in heart cells. Because both AMPK and mitochondrial dysfunction can induce autophagy, it is a niche that must be explored.

Adverse Effects of Rosiglitazone Therapy

Although synthetic ligands of PPARγ, specifically rosiglitazone, have been identified and applied as anti-diabetic agents, they have also been associated with elevated risk of myocardial infarction and adverse cardiovascular events, such as congestive heart failure, and cardiovascular ischemia, morbidity and mortality (Nissen & Wolski, 2007, 2011). In a meta-analysis by Nissen and Wolski in 2007, it was determined that treatment with rosiglitazone significantly increased the risk of myocardial infarctions.

These findings are of great importance because there are more than 23 million people with diabetes in the United States and 300 million world-wide. Cardiovascular disease is the leading cause of death in patients with T2DM, which represents 68% of all causes of mortality in these patients (Nissen & Wolski, 2007).

In a follow-up meta-analysis in 2011, Nissen and Wolski reported a 28-39% increase in the risk of myocardial infarctions after treatment with rosiglitazone. The reason for these adverse side effects has yet to be fully elucidated, but it is currently thought to be due to higher levels of circulating low-density lipoprotein cholesterol, which is increased by 23% after treatment with rosiglitazone (Nissen & Wolski, 2011). In comparative efficacy trials, rosiglitazone raised triglyceride levels and increased low-density lipoprotein cholesterol levels over pioglitazone.

In addition, overexpression of PPARγ, like that induced by TZD treatment, induces cardiac hypertrophy (Festuccia *et al.* 2009). These effects can lead to death, especially in patients already predisposed to congestive heart failure, as both diabetes and congestive heart failure induces alterations in energy metabolism and mitochondrial function (Garnier *et al.* 2003; Spinazzi *et al.* 2012)

CHAPTER 4
RESULTS

Rosiglitazone is a PPARy agonist, which is prescribed to treat Type II Diabetes mellitus due to its insulin sensitizing effects. With more and more diabetic patients taking rosiglitazone, cardiovascular side effects became apparent. This prompted investigations aiming to understand the underlying biological mechanisms by which rosiglitazone affects cardiac function. In this study, we hypothesized that rosiglitazone impairs cellular bioenergetics and cellular quality control mechanisms, thereby ultimately leading to cardiac dysfunction. Specifically, we hypothesized 1) that rosiglitazone impairs mitochondrial function in the heart, thus compromising energy balance in heart cells; and 2) that rosiglitazone suppresses autophagic activity in heart cells, which could lead to disruption of cellular homeostasis and heart remodeling. To test the first hypothesis (section 4.1), we measured the weight of hearts from Fischer 344 rats that had been administered 10mg/kg/day rosiglitazone for 19 days, and determined cardiac mitochondrial respiratory function (indicated by cytochrome *c* oxidase and citrate synthase activity). To complement these analyses, we exposed cultured cardiomyocytes (AC16 cells, a human derived ventricular cardiac cell line) to rosiglitazone and assessed mitochondrial function using enzyme activity assays and high resolution respirometry. To test the second hypothesis (section 4.2), we analyzed the autophagic response in hearts from rosiglitazone treated Fischer 344 rats and AC16 cells by determining the expression of an autophagy marker protein.

In summary, we found that 1) routine respiration and maximal electron transport capacity of the mitochondrial electron transport system were decreased by high concentrations of rosiglitazone *in vitro*, but 2) the activity of the mitochondrial enzyme

cytochrome *c* oxidase was decreased by low concentrations of rosiglitazone *in vitro*, or was not affected at all *in vivo*. Furthermore, we report that 3) autophagic flux was not affected by rosiglitazone *in vivo* and *in vitro*.

Effect of Rosiglitazone on Mitochondrial Function in vivo and in vitro

Effect of Rosiglitazone on Hearts from Fischer 344 Rats

Effect of rosiglitazone administration on heart size in Fischer 344 rats

Fischer 344 rats of three different ages were administered 10mg Rosiglitazone/kg/day for 19 days. At the end of this period the rats were weighed to determine their body weight and subsequently euthanized (see Methods section). In order to determine if rosiglitazone administration had an effect on heart size the heart was collected from each rat after euthanization, flushed with PBS, blotted dry and weighed. For further analysis, heart weight was normalized to body weight (HW/BW, mg g^{-1}, Figure 4-1). Heart weight and body weight increased with age, independent of treatment (Table 4-1; age-effect: $p \leq 0.001$). This increase was significant between ages 5 and 12 months, and 5 and 18 months, but not between ages 12 and 18 months (Table 4-1). However, heart weight normalized to body weight (HW/BW) decreased with age, independent of treatment (age-effect, $p<0.001$; Figure 4-1). Rosiglitazone treatment had no effect on HW/BW compared to controls of the same age (treatment-effect, p=0.502, 5 mo; 0.615, 12 mo; 0.263, 18 mo).

Effect of rosiglitazone administration on mitochondrial enzyme activities in heart from Fischer 344 rats

In order to determine if mitochondrial function in heart tissue of Fischer 344 rats was affected by rosiglitazone administration, we analyzed the enzymatic activity of two mitochondrial enzymes, cytochrome *c* oxidase and citrate synthase, in heart tissue

extracts (Figure 4-2, 4-3 and 4-4). Cytochrome *c* oxidase (COX) is one of the electron and proton transporting enzyme complexes (complex IV) of the electron transport system, and its activity has been used as a marker of mitochondrial function (Campian *et al.* 2007). Citrate synthase (CS) is an enzyme of the Krebs' cycle (citric acid cycle), located in the mitochondrial matrix. It has been shown to correlate with mitochondrial content, and has therefore used as a marker enzyme of this parameter (Spinazzi *et al.* 2012). In order to evaluate the specific activity of COX, its enzymatic activity is commonly normalized to CS activity. Normalizing COX activity, the indicator of mitochondrial function, to CS activity, measure of mitochondrial content, allows us to assess mitochondrial function per mitochondrial unit.

Citrate synthase activity

CS activity in tissue extracts from rat heart was not affected by age or rosiglitazone treatment ($p=0.248$ and $p=0.535$, respectively, Figure 4-2), and there was no interaction effect of age and treatment ($p=0.543$). Specifically, tissue extracts of hearts from 5 months old rats that had received vehicle or rosiglitazone showed an average CS activity of 0.935 ± 0.125 and 0.936 ± 0.0731 µmol/min/mg protein, respectively, and this difference was not statistically significant ($p=0.994$). CS activity did not significantly change in 12 months old rats within the respective treatment groups and was 0.883 ± 0.082 µmol/min/mg protein in vehicle treated rats ($p=0.752$), and 0.894 ± 0.10 µmol/min/mg protein in rosiglitazone treated rats ($p=0.470$), respectively, or in 18 months old rats, which averaged $0.902 \pm 0.0.89$ in vehicle treated rats ($p=0.827$), and 0.828 ± 0.177 µmol/min/mg protein in rosiglitazone treated rats ($p=0.219$). No significant change in CS activity was determined in both vehicle and rosiglitazone treated rats at the age of 18 months compared to 12 months old rats ($p=0.741$, vehicle; $p=0.458$

rosiglitazone). Finally, there was no significant difference in CS activity between vehicle and Rosiglitazone treated rats at any age (p=0.994, age 5 months; p=0.852, age 12 months; p=0.221, age 18 months).

Cytochrome *c* oxidase activity

COX activity in tissue extracts from rat heart was not affected by age or rosiglitazone treatment (p=0.634 and p=0.459, respectively, Figure 4-3), and there was no interaction effect of age and treatment (p=0.190). Specifically, tissue extracts of hearts from 5 months old rats that received vehicle or rosiglitazone had an average COX activity of 0.582 ± 0.176 and 0.607 ± 0.208 µmol/min/mg protein, respectively, and this difference was not statistically significant (p=0.784). COX activity did not significantly change in 12 months old rats within the respective treatment groups, and was 0.456 ± 0.167 µmol/min/mg protein in vehicle treated rats (p=0.290), and 0.615 ± 0.087 µmol/min/mg protein in rosiglitazone treated rats (p=0.928), respectively, or in 18 months old rats, which averaged 0.593 ± 0.137 µmol/min/mg protein in vehicle treated rats (p=0.907), and 0.523 ± 0.218 µmol/min/mg protein in rosiglitazone treated rats (p=0.591). No significant change in COX activity was determined in both vehicle and rosiglitazone treated rats at the age of 18 months compared to 12 months old rats (p=0.332, vehicle; p=0.659, rosiglitazone). Finally, there was no significant difference in COX activity between vehicle and rosiglitazone treated rats at any age (p=0.784, age 5 months; p=0.067, age 12 months; p=0.447, age 18 months).

Cytochrome c oxidase activity normalized to citrate synthase activity

Normalized COX activity, hereafter referred to as normalized COX activity, in tissue extracts from rat heart was not affected by age or rosiglitazone treatment (p=0.860 and p=0.345, respectively, Figure 4-4), and there was no interaction effect of

age and treatment (p=0.386). Specifically, tissue extracts of hearts from 5 months old rats that received vehicle or rosiglitazone had an average normalized COX activity of 0.636 ± 0.215 and 0.655 ± 0.245 µmol/min/mg protein, respectively, and this difference was not statistically significant (p=0.869). Normalized COX activity did not significantly change in 12 months old rats within the respective treatment groups and was 0.522 ± 0.202 µmol/min/mg protein in vehicle treated rats (p=0.496), and 0.700 ± 0.146 µmol/min/mg protein in rosiglitazone treated rats (p=0.893), respectively, or in 18 months old rats, which averaged 0.657 ± 0.133 µmol/min/mg protein in vehicle treated rats (p=0.856), and 0.639 ± 0.267 µmol/min/mg protein in rosiglitazone treated rats (p=0.884). No significant change in normalized COX activity was determined in both vehicle and rosiglitazone treated rats at the age of 18 months compared to 12 months old rats (p=0.516, vehicle; p=0.919, rosiglitazone). There was no significant difference in normalized COX activity between vehicle and rosiglitazone treated rats at any age (p=0.869, age 5 months; p=0.092, age 12 months; p=0.871, age 18 months).

Summary of Analyses of Heart Size and Mitochondrial Function in Fischer 344 Rats

In summary, we found that rosiglitazone administration to Fischer 344 rats had no effect on heart weight and heart weight normalized to body weight. However, heart weight normalized to body weight decreased from 5 to 12 and 18 months of age. Furthermore, neither rosiglitazone administration nor age had an effect on activities of the mitochondrial enzymes cytochrome *c* oxidase and citrate synthase in rat heart.

Effect of Rosiglitazone on Mitochondrial Function in AC16 Cardiomyocytes

In addition to the experiments and analyses on rat heart tissue, we conducted experiments on the effects of rosiglitazone *in vitro*, which allowed manipulation of

rosiglitazone concentrations and exposure times. We used AC-16 cells, which are immortalized human adult ventricular cardiomyocytes, expressing adult cardiomyocyte markers, such as α-cardiac actin and β-myosin heavy chain (Garbern *et al.* 2013). This made them a good *in vitro* complement to the *in vivo* study. We measured mitochondrial respiration and enzymatic activity of two mitochondrial enzymes, cytochrome c oxidase and citrate synthase, using high resolution respirometry (HRR), and spectrophotometric enzyme activity assays, respectively.

Effects of Rosiglitazone on Mitochondrial Enzymatic Activities *in vitro*

In order to determine if the dose of rosiglitazone application has an effect on mitochondrial function in cardiomyocytes, we exposed AC16 cells to four doses (0, 10μM, 100μM, or 200μM) of rosiglitazone for four hours and assessed the activities of two mitochondrial enzymes, cytochrome *c* oxidase and citrate synthase (Figures 4-5, 4-6 and 4-7).

Citrate synthase activity

CS activity in AC16 cell lysates was not affected by rosiglitazone dose ($p=0.249$, Figure 4-5). Specifically, cells exposed to vehicle (0.01% DMSO) showed an average CS activity of 0.568 ± 0.0156 μmol/min/mg protein, cells exposed to 10μM rosiglitazone showed an average CS activity of 0.0318 ± 0.0059 μmol/min/mg protein, cells exposed to 100μM rosiglitazone showed an average CS activity of 0.0468 ± 0.0207 μmol/min/mg protein, and cells exposed to 200μM rosiglitazone showed an average CS activity of 0.0527 ± 0.0125 μmol/min/mg protein. Activities in the rosiglitazone groups were not statistically different from control (0 vs. 10μM: $p=0.196$; 0 vs. 100μM: $p=0.674$; 0 vs. 200μM: $p=0.740$).

Cytochrome *c* oxidase activity

COX activity in AC16 cell lysates was not affected by rosiglitazone dose ($p=0.151$, Figure 4-6). Specifically, cells exposed to vehicle (0.01% DMSO) showed an average COX activity of 0.0324 ± 0.0212 µmol/min/mg protein, cells exposed to 10µM rosiglitazone showed an average COX activity of 0.0097 ± 0.00045 µmol/min/mg protein, cells exposed to 100µM rosiglitazone showed an average COX activity of 0.0165 ± 0.00205 µmol/min/mg protein, and cells exposed to 200µM rosiglitazone showed an average COX activity of 0.0173 ± 0.00451 µmol/min/mg protein. When activities of the rosiglitazone groups were compared to the control group, 10µM rosiglitazone treated cells had a significantly lower COX activity ($p<0.05$), but the other treatment groups were not significantly different (0 vs. 100µM: $p=0.211$; 0 vs. 200µM: $p=0.127$).

Cytochrome c oxidase activity normalized to citrate synthase activity

Normalized COX activity of AC16 cells exposed to rosiglitazone was not affected by the dose of rosiglitazone treatment ($p=0.262$ Figure 4-7). Specifically, cells exposed to vehicle (0.01% DMSO) showed an average normalized COX activity of 0.540 ± 0.212 µmol/min/mg protein, cells exposed to 10µM rosiglitazone showed an average normalized COX activity of 0.310 ± 0.0426 µmol/min/mg protein, cells exposed to 100µM rosiglitazone showed an average normalized COX activity of 0.390 ± 0.126 µmol/min/mg protein, and cells exposed to 200µM rosiglitazone showed an average normalized COX activity of 0.342 ± 0.123 µmol/min/mg protein. Activities in the rosiglitazone groups were not statistically different from control (0 vs. 10µM: $p=0.215$; 0 vs. 100µM: $p=0.151$; 0 vs. 200µM: $p=0.199$).

Effects of Rosiglitazone on Mitochondrial Respiration *in vitro*

In addition to determination of mitochondrial enzyme activity, mitochondrial respiration was measured, using a High Resolution Respirometer. AC16 cells were exposed to rosiglitazone and oxygen consumption of intact cells in culture media was assessed following the exposure. A low (10µM) or a high (200µM) dose of rosiglitazone was applied for a duration of 4 hours or 24 hours (for number of replicates for each treatment see Table 4-2). Each rosiglitazone exposure experiment was accompanied by a control exposure (cell culture media). Based on the titration protocol outlined in the Methods section, the following respiratory states, and flux and coupling control ratios were analyzed and calculated (for definitions refer to Methods section): *Routine respiration* (R; oxygen consumption rate, or oxygen flux, of intact cells in culture media in the absence of inhibitors or uncouplers), *LEAK respiration* (L; oxygen flux in the presence of an inhibitor of the phosphorylation system, e.g. oligomycin), *ETS capacity* (E; oxygen flux in the presence of an uncoupler, e.g. FCCP, which dissipates the mitochondrial membrane potential), *Leak control ratio* (L/E), and *Uncoupling control ratio* (E/R).

Routine respiration: Routine respiration rate under control conditions was 46.1 ± 18.5 and 42.6 ± 15.6 pmol s^{-1} 10^{-6} cells (4 h and 24 hour exposure, respectively; Table 4-2, Figure 4-8). When cells were exposed to 10 µM rosiglitazone for 4 or 24 hours, routine respiration amounted to 50.9 ± 13.1 and 42.5 ± 11.9 pmol s^{-1} 10^{-6} cells, respectively. Cells exposed to 200 µM rosiglitazone for 4 or 24 hours had a routine respiration rate of 24.5 ± 13. 7 and 27.0 ± 3.2 pmol s^{-1} 10^{-6} cells, respectively. There was no overall effect of duration of exposure on routine respiration (p=0.557), and duration of exposure had no effect on routine respiration within each dose group

(p=0.607, 0.408, and 0.798 for 0, 10, and 200 µM rosiglitazone, respectively). However, there was an overall significant effect of rosiglitazone dose on routine respiration (p=0.007). That is, the overall mean of routine respiration in cells exposed to 200 µM rosiglitazone (4h and 24 h combined) was lower than the overall mean of routine respiration of control cells (4h and 24h combined; p=0.012), and of cells exposed to 10 µM rosiglitazone (4h and 24h combined; p=0.012), independent of duration of the exposure. Routine respiration of control cells (4h and 24h combined) and cells exposed to 10 µM rosiglitazone (4h and 24h combined) were not statistically different (p=0.704). When differences between doses within the same exposure duration were analyzed, routine respiration was decreased in cells treated for 4 hours with 200 µM compared to 10 µM rosiglitazone (p=0.025) and to control cells (p=0.037), but not when cells were treated for 24 hours (p=0.248, 200 µM – 10 µM; p=0.239, 200 µM – control). Routine respiration of control cells and cells treated with 10 µM rosiglitazone did not differ from each other, independent of duration of exposure (4h: p=0.592, 24h: p=0.985). Finally, there was no interaction effect of dose x duration (p=0.741).

LEAK respiration: LEAK respiration (LEAK; L) was measured after the inhibition of the phosphorylation system through the ATP synthase inhibitor oligomycin. This inhibition increases the electrochemical proton gradient across the inner mitochondrial membrane. Oxygen flux is depressed to a level determined by proton leak. LEAK respiration in AC16 cells was not affected by rosiglitazone (dose effect: p=0.246) or duration of exposure to vehicle or rosiglitazone (duration effect: p=0.973), and there was no interaction affect between these factors (p=0.796) (Figure 4-9). Specifically, the overall means of LEAK respiration in cells exposed to 0, 10 and 200 µM rosiglitazone

(4h and 24 h combined) did not statistically differ from each other, independent of duration of the exposure (p=0.983, 0-10 µM; p=0.305, 0-200 µM; p=0.314, 10-200 µM). When differences between doses within the same exposure duration was analyzed, LEAK respiration was unchanged in cells treated for 4 hours with 10 or 200 µM compared to control cells (p=0.802, 0-10 µM; p=0.282, 0-200 µM; p=0.456, 10-200 µM, Table 4-2). LEAK respiration was also unaffected in cells treated for 24 hours with 10 or 200 µM rosiglitazone compared to control cells (p=0.763, 0-10 µM; p=0.760, 0-200 µM; p=0.794, 10-200 µM).

ETS capacity: The maximal electron transport capacity (ETS capacity; E) is experimentally induced by titration of an uncoupler (FCCP), and is characterized by the collapse of the mitochondrial membrane potential across the inner mitochondrial membrane. ETS capacity in AC16 cells was not affected by duration of exposure to vehicle or rosiglitazone (p=0.558), but was significantly decreased by rosiglitazone (dose effect: p=0.001; Figure 4-10). Specifically, the overall mean of ETS capacity in cells exposed to 200 µM rosiglitazone (4h and 24 h combined) was lower than the overall mean of ETS capacity of control cells (4h and 24h combined; p=0.004), and of cells exposed to 10 µM rosiglitazone (4h and 24h combined; p=0.002), respectively, independent of duration of the exposure (Table 4-2). ETS capacity of control cells (4h and 24h combined) and cells exposed to 10 µM rosiglitazone (4h and 24h combined) were not statistically different (p=0.261). When differences between doses within the same exposure duration was analyzed, ETS capacity was decreased in cells treated for 4 hours with 200 µM compared to 10 µM rosiglitazone (p=0.018) and to control cells (p=0.042). ETS capacity in cells treated for 24 hours with 200 µM rosiglitazone was

significantly or tended to be lower compared to control (p=0.048) and cells exposed to 10 µM rosiglitazone (p=0.054), respectively. ETS capacity of control cells and cells treated with 10 µM rosiglitazone did not differ from each other, independent of duration of exposure (4h: p=0.279, 24h: p=0.623). Finally, there was no interaction effect between duration of exposure and rosiglitazone dose (p=0.894).

LEAK control ratio: The Leak control ratio (LCR; L/E) is an index of uncoupling at constant ETS capacity, and indicates how much LEAK respiration is contributing to the overall capacity of the electron transport system. LCR in AC16 cells was not affected by duration of exposure to vehicle or rosiglitazone (p=0.379), but was significantly increased by rosiglitazone (dose effect: p=0.004; Figure 4-11). Specifically, independent of duration of the exposure, the overall mean of LCR in cells exposed to 200 µM rosiglitazone (4h and 24 h combined) was higher than the overall mean of LCR in control cells (4h and 24h combined; p=0.016), and of cells exposed to 10 µM rosiglitazone (4h and 24h combined; p=0.005), respectively (Table 4-2). LCR of control cells (4h and 24h combined) and cells exposed to 10 µM rosiglitazone (4h and 24h combined) were not statistically different (p= 0.218). When differences between doses within the same exposure duration was analyzed, LCR was not significantly different in cells treated for 4 hours independent of rosiglitazone dose (p=0.258, 0-10 µM; p=0.266, 0-200µM; p=0.093, 10 µM-200 µM). LCR in cells treated for 24 hours with 200 µM rosiglitazone was significantly elevated compared to control (p=0.039) and cells exposed to10 µM rosiglitazone (p=0.036), respectively. LCR of control cells and cells treated with 10 µM rosiglitazone did not differ from each other after 24 h of exposure

(p=0.549). Finally, there was no interaction effect between duration of exposure and rosiglitazone dose (p=0.724).

Routine control ratio: The routine control ratio (R/E) is used to evaluate how close routine respiration operates to ETS capacity. R/E in AC16 cells was not affected by duration of exposure to vehicle or rosiglitazone (p=0.609), but was significantly decreased by rosiglitazone (dose effect: p=0.029; Figure 4-12). Specifically, independent of duration of the exposure, the overall mean of R/E in cells exposed to 200 µM rosiglitazone (4h and 24 h combined) was higher than the overall mean of R/E of cells exposed to 10 µM rosiglitazone (4h and 24h combined; p=0.025). R/E of control cells (4h and 24h combined) was not statistically different from cells exposed to 10 µM rosiglitazone (4h and 24h combined; p=0.150), and 200 µM rosiglitazone (4h and 24h combined; p=0.148). When differences between doses within the same exposure duration was analyzed, R/E was increased in cells treated for 24 hours with 200 µM compared to 10 µM rosiglitazone (p=0.019), while there were no statistical differences between the other treatments (4h exposure: p=0.459, 0-10 µM; p=0.914, 0-200 µM; p=0.508, 10-200 µM; 24h exposure: p=0.082, 0-200 µM, p=0.211, 0-10 µM) (Table 4-2). Finally, there was no interaction effect between duration of exposure and rosiglitazone dose (p=0.255).

Summary of Analyses of Mitochondrial Function in AC16 Cells

In summary, we found that, independent of duration of exposure, routine respiration and ETS capacity of AC16 cells were decreased when cells were exposed to 200 µM rosiglitazone, while LEAK respiration was unaffected. This was reflected in an increase in LEAK control ratio (LCR; L/E) and routine control ratio (RCR; R/E). Analysis of mitochondrial enzymes showed no effect of rosiglitazone on mitochondrial function as

determined by activities of COX and CS. COX activity appeared to be depressed by exposure to 10µM rosiglitazone, but the effect was removed when COX activity was normalized to CS activity.

Effect of Rosiglitazone on Autophagy in vivo and in vitro

In this part of the study, we investigated the effect of rosiglitazone administration on autophagy *in vivo* in rat heart, and *in vitro* in AC16 cardiomyocytes. We measured in heart tissue extracts and cell lysates, respectively, protein expression of the autophagy marker MAP-LC3 (microtubule-associated protein light chain 3). LC3 is essential for the expansion of the early autophagosome, and becomes posttranslationally modified. Pre-LC3 is processed by the autophagy protein Atg4 to its cytosolic form, LC3-I. LC3-I is then activated by Atg7, transferred to Atg3 and lipidated to its membrane bound form, LC3-II, localized to the preautophagosome structure and the autophagosomes (Abeliovich *et al.* 2000). Its posttranslational modification from cytosolic LC3-I to membrane-bound LC3-II makes it a useful marker of autophagy (Rubinsztein *et al.* 2009). In this study, protein expression of LC3-I and LC3-II was analyzed in rat heart tissue extracts, and calculated the ratio of LC3-II/I as a measure of autophagic activity in the heart. However, these measures represent only a snapshot of autophagic activity in the biological material fixed at a given time. Therefore the investigation of autophagy in rat cardiac tissue was complemented with *in vitro* experiments. Here, AC16 cells were exposed to rosiglitazone in the presence and absence of bafilomycin A1 (BafA1), a lysosomal inhibitor (Rubinsztein *et al.* 2009). BafA1 inhibits the fusion of the autophagosome with the lysosome, which leads to an accumulation of the autophagosome-bound form LC3-II. The difference of accumulated LC3-II between

BafA1-treated and BafA1-untreated cells can then be utilized to determine the autophagic flux.

We found that autophagy, using the protein expression of LC3-II and LC3-I as an indicator, was not affected by age (p=0.901) or treatment (p=0.755) in the hearts of Fischer 344 rats supplemented with 10mg/kg/day rosiglitazone for 19 days (Figure 14-13). Specifically 5 months of age did not significantly differ from 12 months or 18 months (p=0.923 and p=0.967, respectively) and 12 months did not significantly differ from 18 months (p=0.953). Within the vehicle treatment 5 months did not differ from 12 months or 18 months (p=0.791 and p=0.854, respectively) and 12 months did not significantly differ from 18 months (p=0.876). Similar results were obtained in the rosiglitazone treated group, where 5 months did not differ from 12 months or 18 months (p=0.964 and p=0.891, respectively) and 12 months did not significantly differ from 18 months (p=0.975).

We next analyzed autophagic flux in the presence of rosiglitazone in AC16 cells, by exposing cells to fed conditions (control), starvation (used to induce autophagy through nutrient deprivation) and varying doses of rosiglitazone, and then treating a duplicate sample of cells with BafA1. BafA1 is a proton pump inhibitor, which prevents the fusion of the autophagosome with the lysosome by neutralizing the lysosomal pH, causes the accumulation of autophagosomes (Rubinsztein *et al.* 2009). Because the final degradation of the autophagosomes and their contents is prevented, the autophagosomal membrane-bound form of the autophagy marker protein LC3-II accumulates. LC3-II accumulation can then be utilized to determine the autophagic flux

by calculating the difference of LC3-II protein level between the cells treated without and the cells treated with BafA1 within the same treatment.

We first assessed whether autophagy is inducible in the AC16 cell via starvation. Although there is an increase in autophagosome formation in the starved cells compared to over control cells with mean LC3II/LC3I ratios of 0.568 ± 0.310 and 1.582 ± 0.237, respectively, and LC3II/LC3I ratios of 3.086 ± 1.614 and 6.115 ± 3.89 in BafA1-treated control and starved cells, respectively, the overall effect of 4 hours of starvation was not statistically significant (p=0.150).

We next assessed autophagic flux in AC16 cells exposed to rosiglitazone by calculating the fold-increase caused by addition of BafA (LC3-II/I ratio of cells in the presence of BafA1divided by the value in the absence of BafA1). Treatment with rosiglitazone did not have an effect on autophagic flux (p=0.219; Figure 14-14). Specifically, LC3-II/I ratio increased 4.71 ± 2.12 fold in control cells, 10.05 ± 7.40 in cells treated with 10μM rosiglitazone, 19.16 ± 12.92 in cells treated with 100μM rosiglitazone, and 7.66 ± 4.15 in cells treated with 200μM rosiglitazone. Comparisons between the autophagic flux in cells treated with different doses of rosiglitazone were not statistically significant (0-10μM: p=0.860; 0-100μM: p=0.305; 0-200μM: p= 0.884; 10-100μM: p=0.674; 10-200μM: p=0.749; 100-200μM: p=0.460; Figure 14-14 D).

In summary, autophagy was not affected by treatment with rosiglitazone *in vivo* or *in vitro*. Little research has been reported on the effects of PPARγ stimulation, via TZD's or otherwise, on autophagy, to corroborate or contradict our findings.

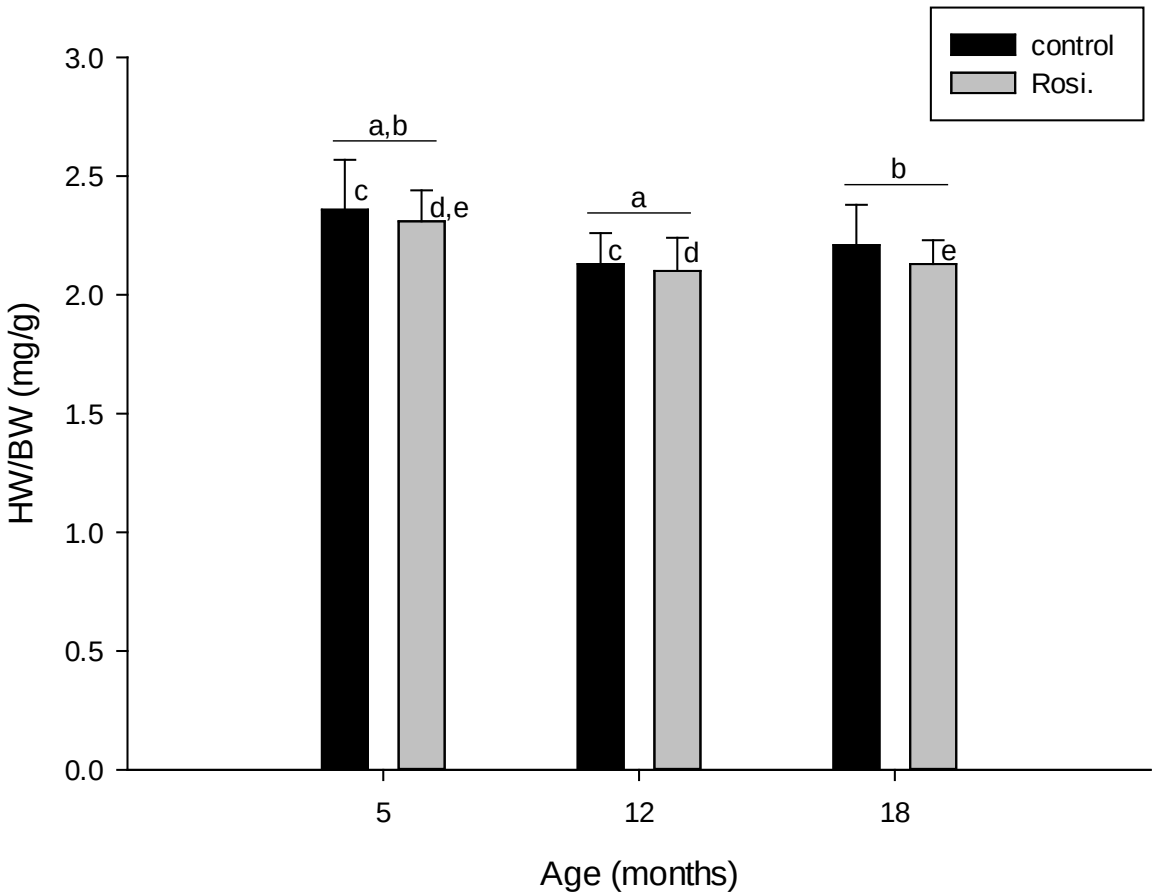

Figure 4-1. Heart weight (HW, mg) normalized to body weight (BW, g) of Fischer 344 rats age 5, 12 and 18 months that received rosiglitazone or vehicle (control) for 19 days prior to euthanization. (for number of animals per group refer to Methods section). Data are represented as mean ± SD. Same indices indicate significant difference between groups. a: $p< 0.001$, b: $p=0.004$, c: $p=0.005$, d: $p=0.014$, e: $p=0.038$.

Table 4-1. Heart (HW) and body weight (BW) and heart weight normalized to body weight (HW/BW) of Fischer 344 rats aged 5, 12 and 18 months, rats were treated for 19 days with either vehicle (control) or 10 mg rosiglitazone/kg/day (rosi). Data are represented as mean ± SD. Superscripts indicate significant difference between groups with a-h: p≤ 0.001, i: p=0.005, k: p=0.014, l: p=0.038, with p ≤ 0.05 considered significant.

Age (mo)	Treatment	n	HW	BW	HW/BW
5	control	8	843 ± 60 [a,b]	358 ± 23 [e,f]	2.36 ± 0.2 [i]
5	rosi	8	814 ± 93 [c,d]	353 ± 41 [g,h]	2.31 ± 0.13 [k,l]
12	control	11	996 ± 63 [a]	468 ± 27 [e]	2.13 ± 0.13 [i]
12	rosi	9	978 ± 55 [c]	467 ± 15 [g]	2.10 ± 0.14 [k]
18	control	10	985 ± 111 [b]	446 ± 39 [f]	2.21 ± 0.17
18	rosi	8	1004 ± 67 [d]	472 ± 31 [h]	2.13 ± 0.1 [l]

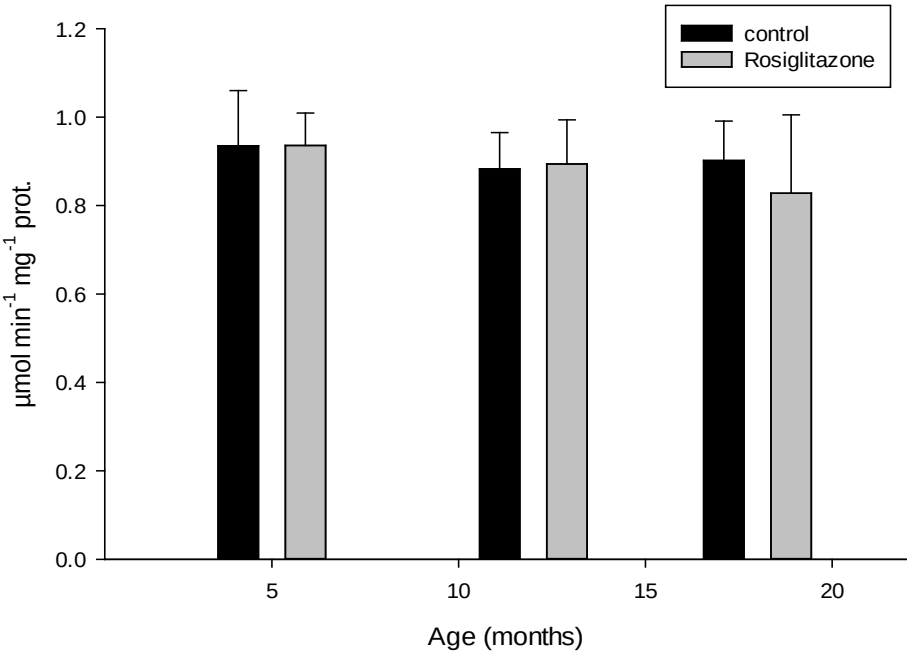

Figure 4-2. Enzymatic activity of Citrate Synthase (CS) (µmol min^{-1} mg^{-1} protein) in tissue extracts of hearts from Fischer 344 rats age 5, 12 and 18 months that received rosiglitazone or vehicle (control) for 19 days prior to euthanization (for number of animals per group refer to Methods section). Data are represented as mean ± SD.

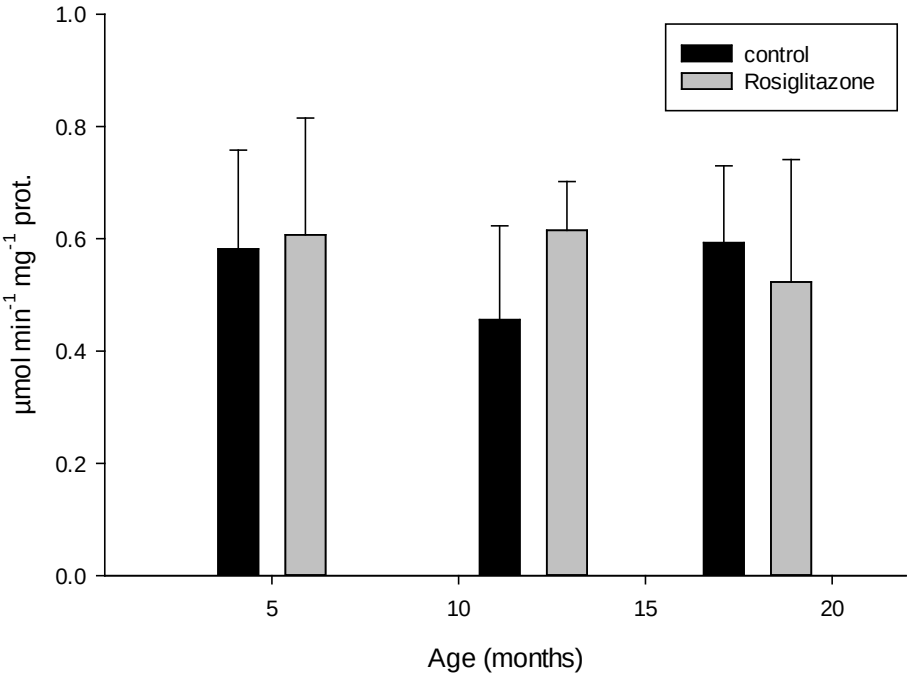

Figure 4-3. Enzymatic activity of Cytochrome c Oxidase (COX) (µmol min^{-1} mg^{-1} protein) in tissue extracts of hearts from Fischer 344 rats age 5, 12 and 18 months that received rosiglitazone or vehicle (control) for 19 days prior to euthanization. (for number of animals per group refer to Methods section). Data are represented as mean ± SD.

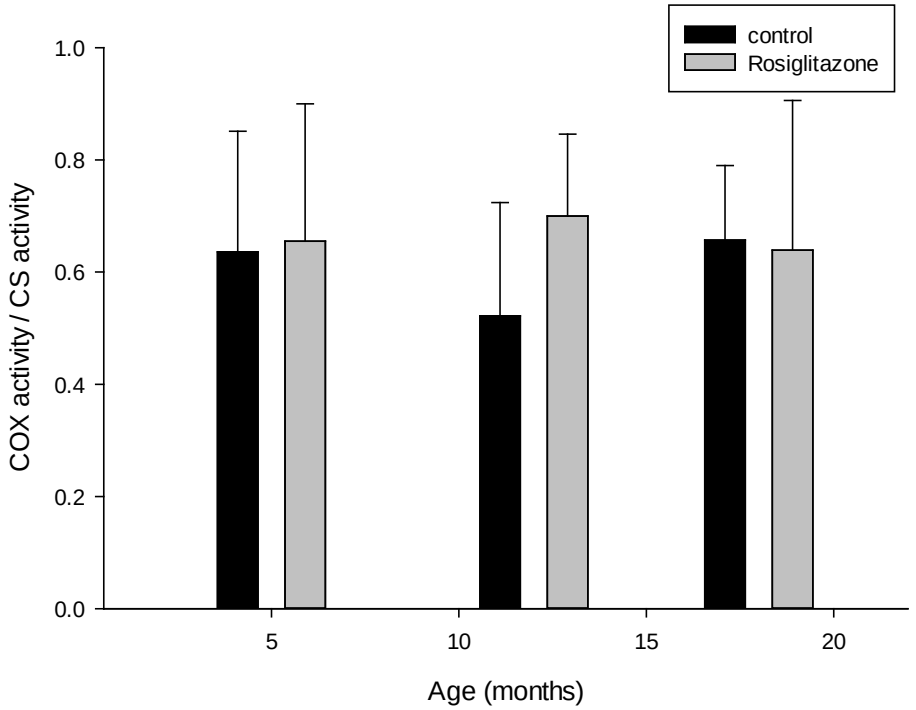

Figure 4-4. COX activity normalized to CS activity in tissue extracts of hearts from Fischer 344 rats age 5, 12 and 18 months that received rosiglitazone or vehicle (control) for 19 days prior to euthanization. (for number of animals per group refer to Methods section). Data are represented as mean ± SD.

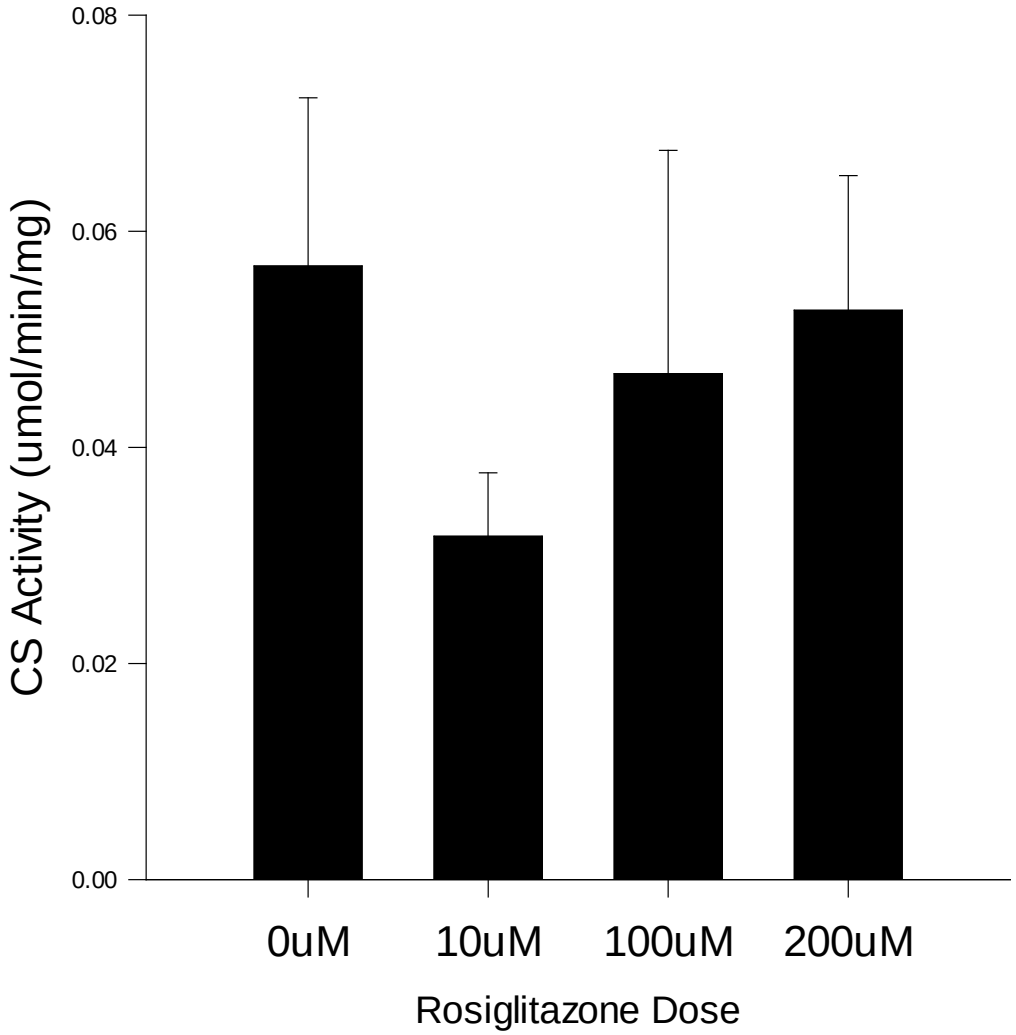

Figure 4-5. Enzymatic activity of Citrate Synthase (CS) (μmol min^{-1} mg^{-1} protein) in AC16 cell that were exposed to rosiglitazone or vehicle (control) for 4 hours prior to cell lysis (for number of experiments per group refer to Methods section). Data are represented as mean ± SD. Same indices indicate significant difference between groups.

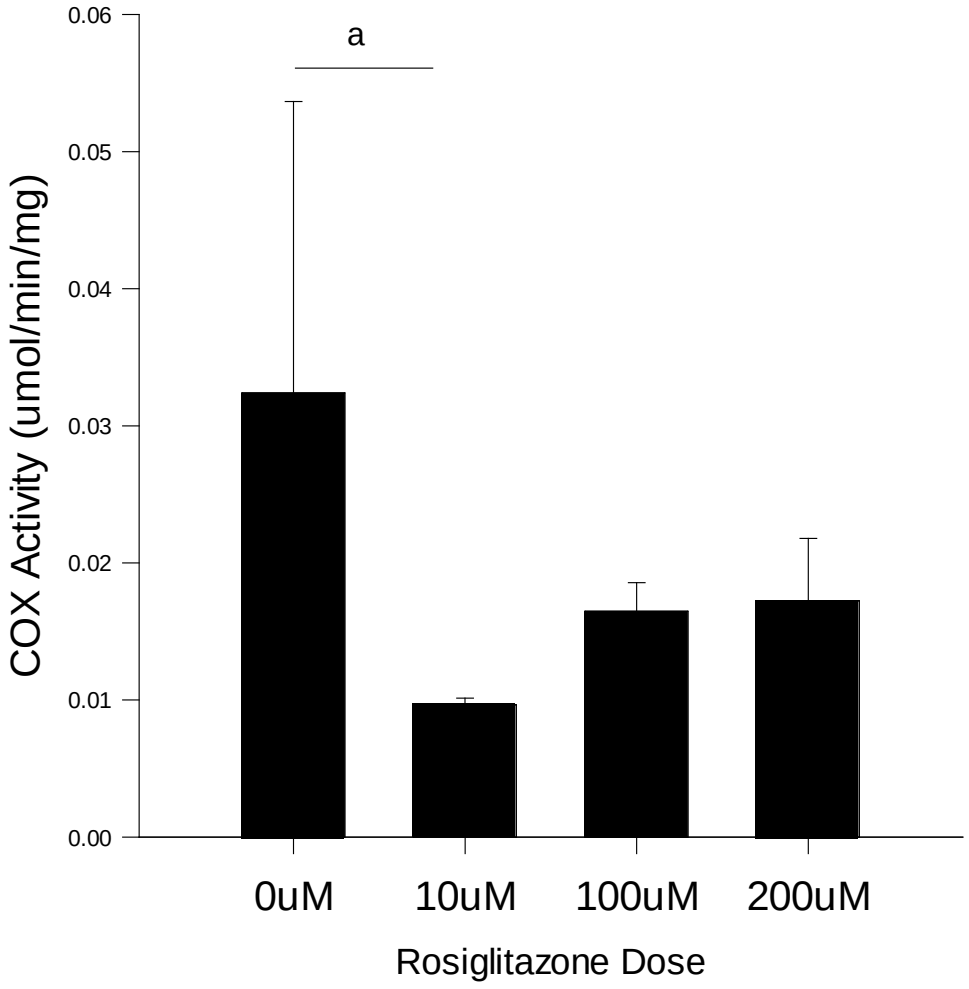

Figure 4-6. COX activity in AC16 cell that were exposed to rosiglitazone or vehicle (control) for 4 hours prior to cell lysis (for number of experiments per group refer to Methods section). Data are represented as mean ± SD. Same indices indicate significant difference between groups.

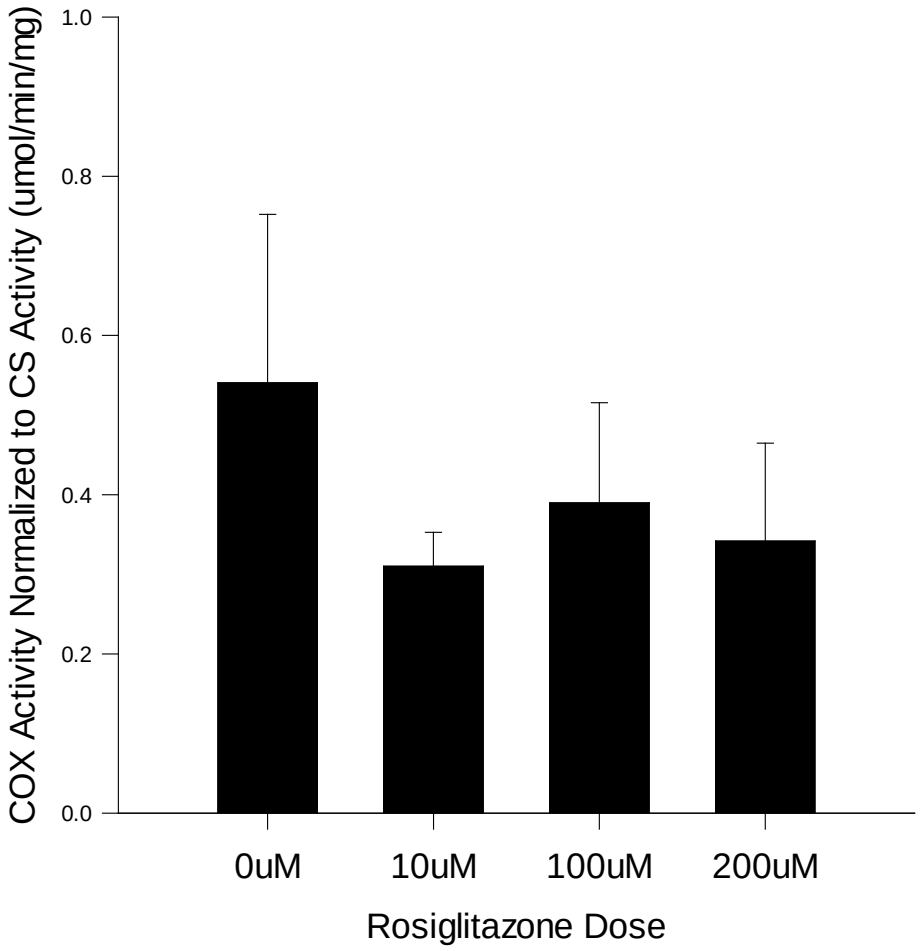

Figure 4-7. COX activity normalized to CS activity in AC16 cell that were exposed to rosiglitazone or vehicle (control) for 4 hours prior to cell lysis (for number of experiments per group refer to Methods section). Data are represented as mean ± SD. Same indices indicate significant difference between groups.

Table 4-2. Oxygen flux (pmol s^{-1} 10^{-6} cells) of AC16 cells under control conditions (CTRL) or after exposure to rosiglitazone (10 or 200 uM) for 4 or 24 hours. Oxygen flux measured as: Routine respiration (Routine), LEAK respiration (LEAK), electron transport capacity (ETS). LEAK Control Ratio (LEAK/ETS; L/E) and Routine Control Ratio (Routine/ETS; R/E) were calculated from indicated oxygen flux. Data represent mean ± standard deviation. n: number of replicates indicates independent replication of experiment

Condition	n	Routine	LEAK	ETS	L/E	R/E
CTRL – 4 h	10	46.1 ± 18.5	27.2 ± 14.4	74.1 ± 33.3	0.381 ± 0.118	0.646 ± 0.111
CTRL – 24 h	10	42.6 ± 15.6	24.3 ± 6.7	72.6 ± 27.3	0.379 ± 0.164	0.614 ± 0.147
10μM Rosi. – 4h	4	50.9 ± 13.1	25.7 ± 4.6	91.0 ± 20.3	0.288 ± 0.056	0.557 ± 0.065
10μM Rosi. – 24h	5	42.5 ± 11.9	26.0 ± 5.8	79.7 ± 18.2	0.334 ± 0.078	0.532 ± 0.070
200μM Rosi. – 4h	5	24.5 ± 13.7	18.2 ± 11.8	39.5 ± 23.8	0.494 ± 0.194	0.639 ± 0.119
200μM Rosi – 24h	4	27.0 ± 3.2	20.5 ± 3.8	36.2 ± 7.3	0.579 ± 0.132	0.760 ± 0.112

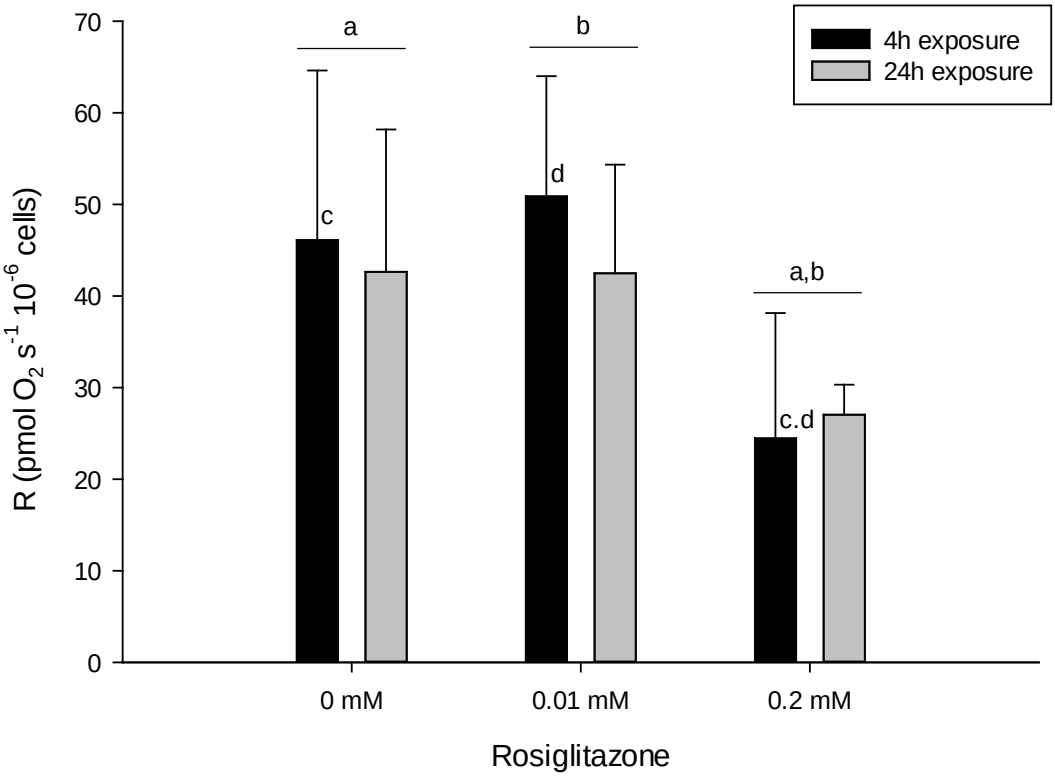

Figure 4-8. Routine respiration of AC16 cells measured in pmol s^{-1} 10^{-6} cells, compared between two exposure durations (4 hours and 24 hours) and three doses of rosiglitazone (0 μM, 10 μM, and 200 μM). Data are represented as mean ± SD. Same indices indicate significant difference. a: p=0.012, b: p=0.012, c: p=0.037, d" p=0.025.

Table 4-3. Statistical analysis of differences between routine respiration rates of AC16 cells under control conditions or after exposure to rosiglitazone (10 or 200 μM) for 4 or 24 hours. p-values were determined using Two-way ANOVA and *post hoc* analysis. Statistical difference was considered significant with $p \leq 0.05$.

Treatment groups compared	p-value
Dose effect	0.007
Time effect*	0.557
Dose x Time* interaction	0.741
0 – 10 μM Rosiglitazone	0.704
0 – 200 μM Rosiglitazone	0.012
10 – 200 μM Rosiglitazone	0.012
4h-Control / 24h-Control	0.607
4h-10 μM Rosiglitazone / 24h-10 μM Rosiglitazone	0.408
4h-200 μM Rosiglitazone / 24h-200 μM Rosiglitazone	0.798
4h: Control / 10 μM Rosiglitazone	0.592
4h: Control / 200 μM Rosiglitazone	0.037
4h: 10 μM Rosiglitazone / 200 μM Rosiglitazone	0.025
24h: Control / 10 μM Rosiglitazone	0.985
24h: Control / 200 μM Rosiglitazone	0.239
24h: 10 μM Rosiglitazone / 200 μM Rosiglitazone	0.248

*: time of exposure (duration of exposure)

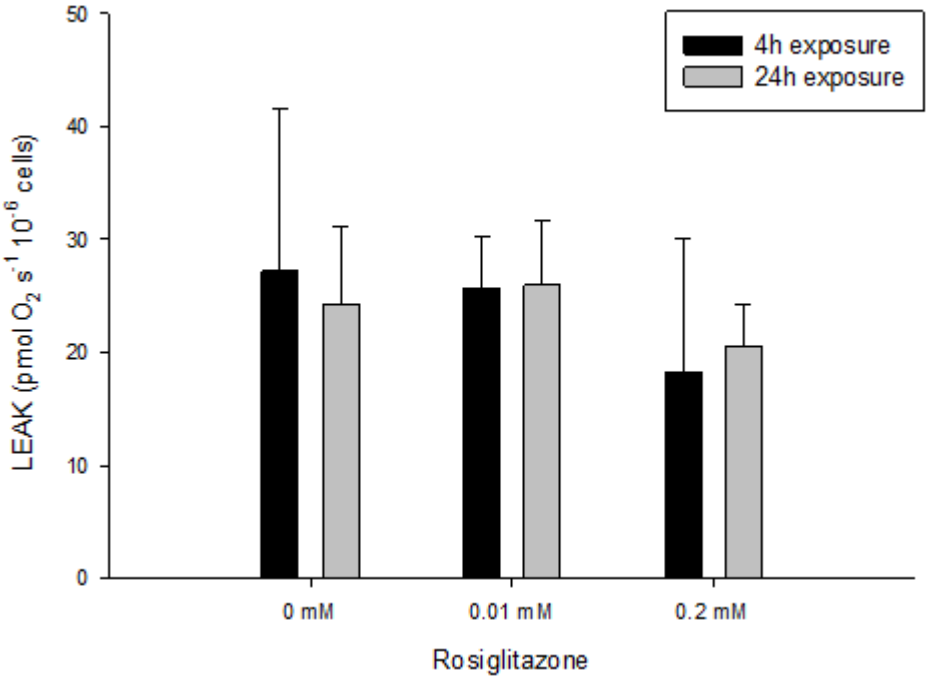

Figure 4-9. LEAK respiration of AC16 cells measured in measured in pmol s^{-1} 10^{-6} cells, compared between two exposure durations (4 hours and 24 hours) and three doses of rosiglitazone (0 µM, 10 µM, and 200 µM). Data are represented as mean ± SD.

Table 4-4. Statistical analysis of differences between LEAK respiration rates of AC16 cells under control conditions or after exposure to rosiglitazone (10 or 200 μM) for 4 or 24 hours. p-values were determined using Two-way ANOVA and *post hoc* analysis. Statistical difference was considered significant with $p \leq 0.05$.

Treatment groups compared	p-value
Dose effect	0.246
Time effect*	0.973
Dose x Time* interaction	0.796
0 – 10 μM Rosiglitazone	0.983
0 – 200 μM Rosiglitazone	0.305
10 – 200 μM Rosiglitazone	0.314
4h: Control / 10 μM Rosiglitazone	0.802
4h: Control / 200 μM Rosiglitazone	0.282
4h: 10 μM Rosiglitazone / 200 μM Rosiglitazone	0.456
24h: Control / 10 μM Rosiglitazone	0.763
24h: Control / 200 μM Rosiglitazone	0.760
24h: 10 μM Rosiglitazone / 200 μM Rosiglitazone	0.794

*: time of exposure (duration of exposure)

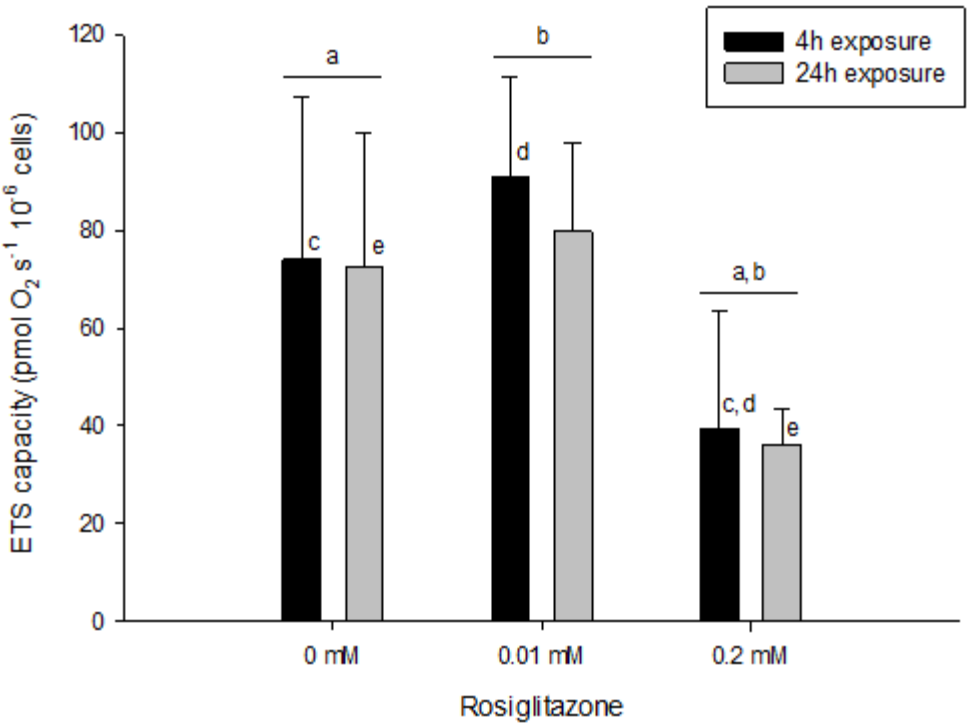

Figure 4-10. ETS respiration of AC16 cells measured in pmol s^{-1} 10^{-6} cells, compared between two exposure durations (4 hours and 24 hours) and three doses of rosiglitazone (0 μM, 10 μM, and 200 μM). Data are represented as mean ± SD. Same indices indicate significant difference. a: p=0.004, b: p=0.002, c: p=0.042, d: p=0.018, e: p=0.048.

Table 4-5. Statistical analysis of differences between electron transport capacity (ETS) of AC16 cells under control conditions or after exposure to rosiglitazone (10 or 200 μM) for 4 or 24 hours. p-values were determined using Two-way ANOVA and post hoc analysis. Statistical difference was considered significant with $p \leq 0.05$.

Treatment groups compared	p-value
Dose effect	0.246
Time effect*	0.973
Dose x Time* interaction	0.796
0 – 10 μM Rosiglitazone	0.983
0 – 200 μM Rosiglitazone	0.305
10 – 200 μM Rosiglitazone	0.314
4h: Control / 10 μM Rosiglitazone	0.802
4h: Control / 200 μM Rosiglitazone	0.282
4h: 10 μM Rosiglitazone / 200 μM Rosiglitazone	0.456
24h: Control / 10 μM Rosiglitazone	0.763
24h: Control / 200 μM Rosiglitazone	0.760
24h: 10 μM Rosiglitazone / 200 μM Rosiglitazone	0.794

*: time of exposure (duration of exposure)

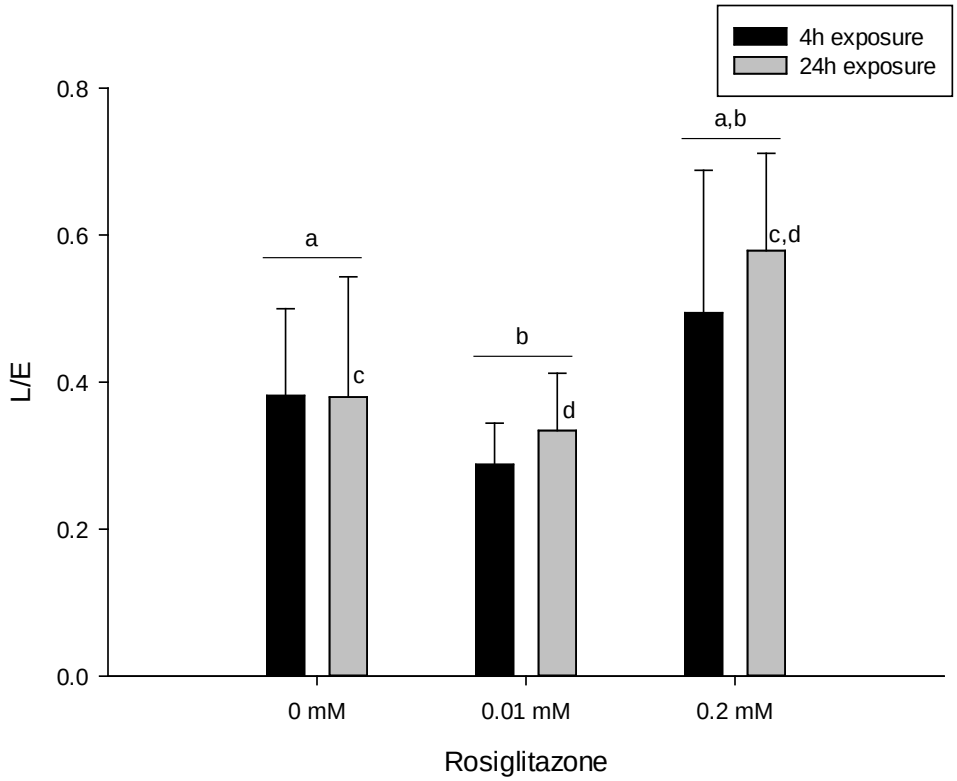

Figure 4-11. Leak control ratio (L/E) of AC16 cells compared between two exposure durations (4 hours and 24 hours) and three doses of rosiglitazone (0 μM, 10 μM, and 200 μM). Data are represented as mean ± SD. Same indices indicate significant difference. a: p=0.004, b: p=0.002, c: p=0.042, d: p=0.018, e: p=0.048.

Table 4-6. Statistical analysis of differences between LEAK Control Ratio (L/E) of AC16 cells under control conditions or after exposure to rosiglitazone (10 or 200 μM) for 4 or 24 hours. p-values were determined using Two-way ANOVA and post hoc analysis. Statistical difference was considered significant with $p \leq 0.05$.

Treatment groups compared	p-value
Dose effect	0.004
Time effect*	0.379
Dose x Time* interaction	0.724
0 – 10 μM Rosiglitazone	0.218
0 – 200 μM Rosiglitazone	0.016
10 – 200 μM Rosiglitazone	0.005
4h: Control / 10 μM Rosiglitazone	0.258
4h: Control / 200 μM Rosiglitazone	0.266
4h: 10 μM Rosiglitazone / 200 μM Rosiglitazone	0.093
24h: Control / 10 μM Rosiglitazone	0.549
24h: Control / 200 μM Rosiglitazone	0.039
24h: 10 μM Rosiglitazone / 200 μM Rosiglitazone	0.036

*: time of exposure (duration of exposure)

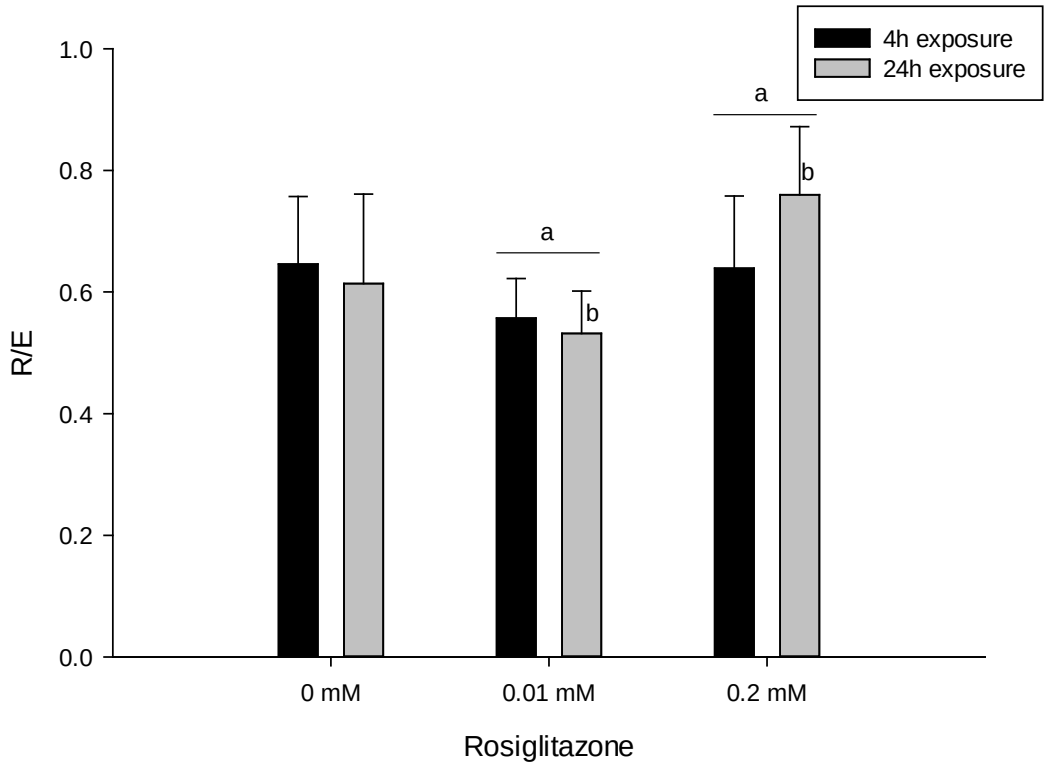

Figure 4-12. Routine control ratio (Routine/ETS, R/E) of AC16 cells compared between two exposure durations (4 hours and 24 hours) and three doses of rosiglitazone (0 μM, 10 μM, and 200 μM). Data are represented as mean ± SD. Same indices indicate significant difference. a: p=0.025, b: p=0.019.

Table 4-7. Statistical analysis of differences between Respiratory Control Ratio (R/E) of AC16 cells under control conditions or after exposure to rosiglitazone (10 or 200 μM) for 4 or 24 hours. p-values were determined using Two-way ANOVA and post hoc analysis. Statistical difference was considered significant with $p \leq 0.05$.

Treatment groups compared	p-value
Dose effect	0.029
Time effect*	0.609
Dose x Time* interaction	0.255
0 – 10 μM Rosiglitazone	0.150
0 – 200 μM Rosiglitazone	0.148
10 – 200 μM Rosiglitazone	0.025
4h: Control / 10 μM Rosiglitazone	0.459
4h: Control / 200 μM Rosiglitazone	0.914
4h: 10 μM Rosiglitazone / 200 μM Rosiglitazone	0.508
24h: Control / 10 μM Rosiglitazone	0.211
24h: Control / 200 μM Rosiglitazone	0.082
24h: 10 μM Rosiglitazone / 200 μM Rosiglitazone	0.019

*: time of exposure (duration of exposure)

A.

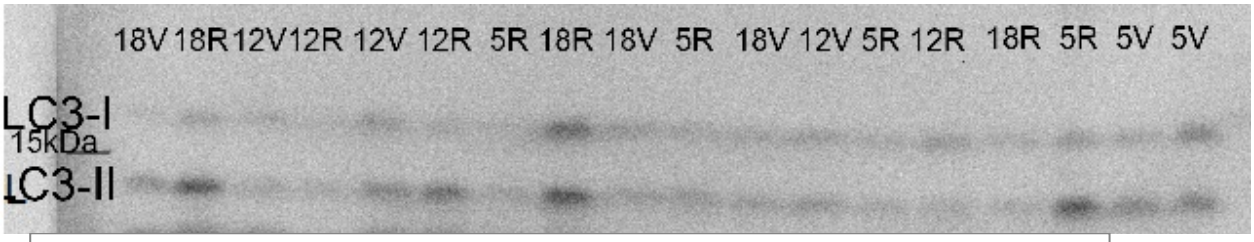

B.

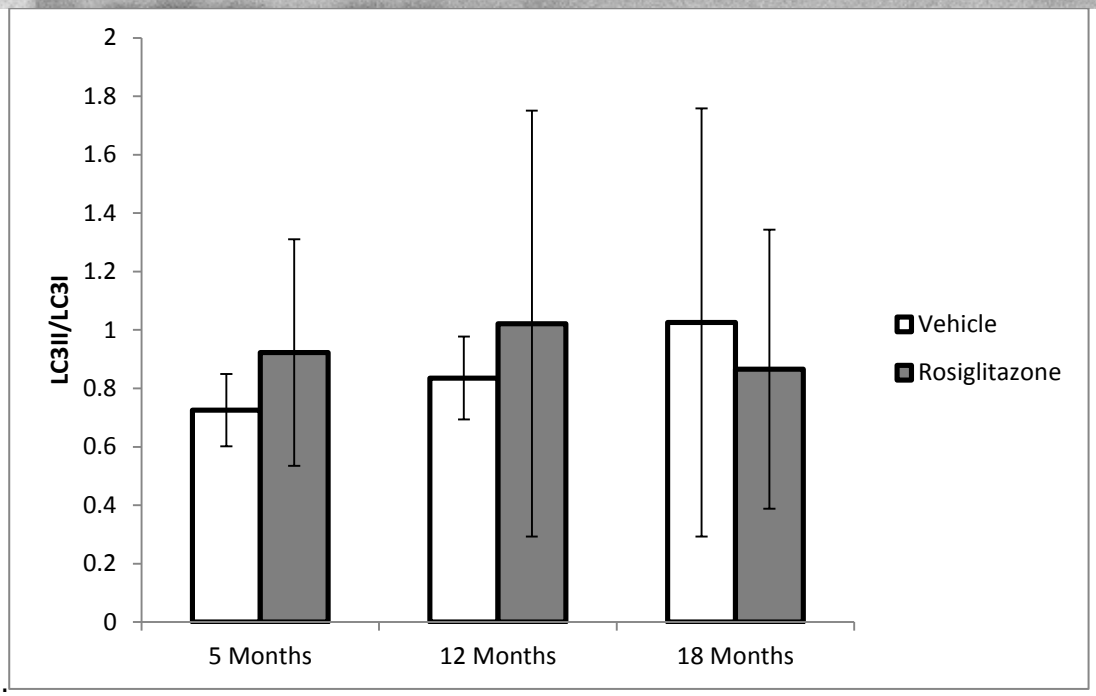

Figure 4-13. Protein expression of LC3 I and II in rat heart tissue extracts. A.) Western Blot of LC3-I and LC3-II. Lanes annotated with months of age (5, 12, and 18) and treatment (R: rosiglitazone; V: vehicle). B.) Ratio of LC3II/LC3I in rat cardiac tissue (n=3 per treatment group). Data are represented as mean ± SD.

A.

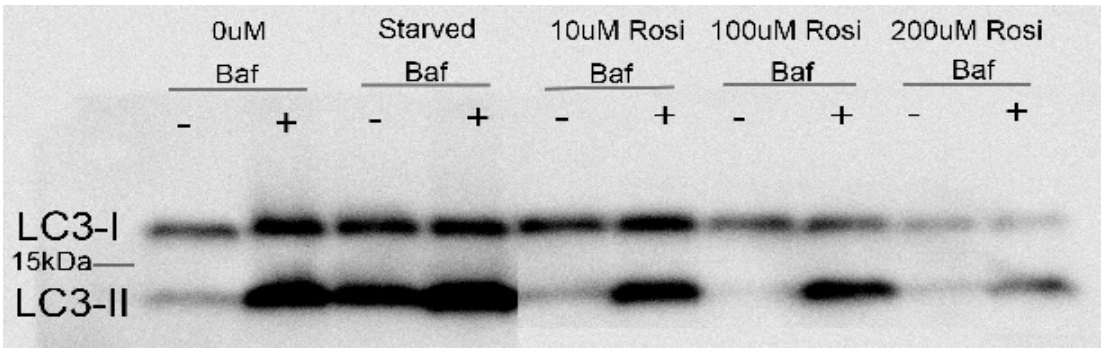

B.

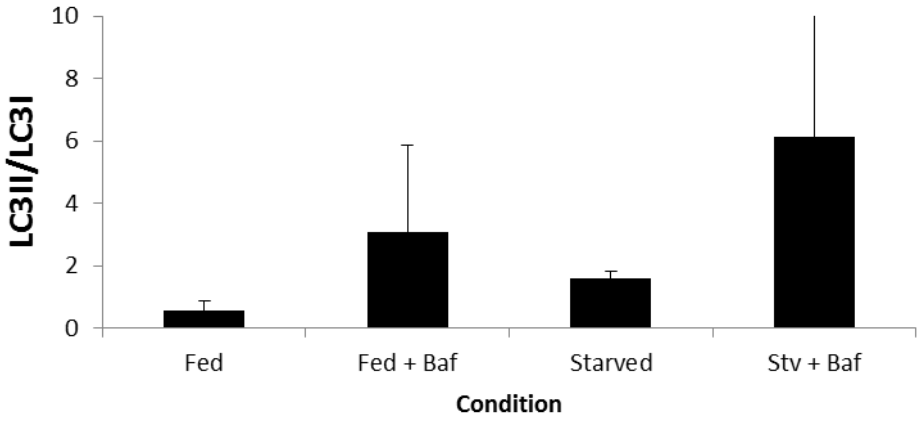

Figure 4-14. Protein expression of LC3 I and II in AC16 cell lysates. A.) Western Blot of LC3-I and II in AC16 cells that had been exposed to varying doses of rosiglitazone for 4 hours (0, 10, 100, 200 uM) or that had been starved for the same duration, in the absence or presence of 50 nM bafilomycin A1. B.) Ratio of LC3II/LC3I in AC16 cell lysate (n=3 per treatment group). Data are represented as mean ± SD. Autophagy is inducible in AC16 cells by starvation.

C.

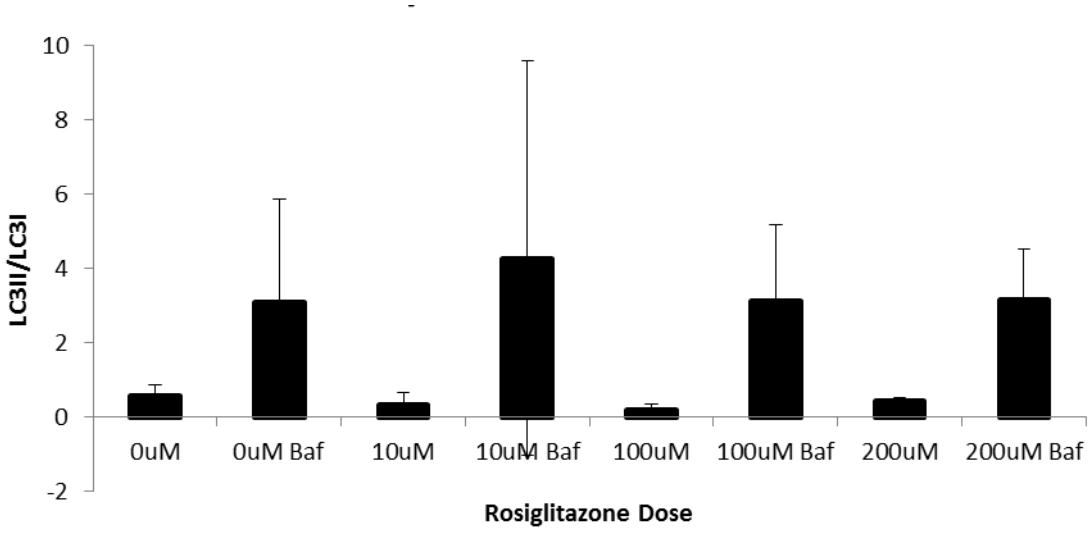

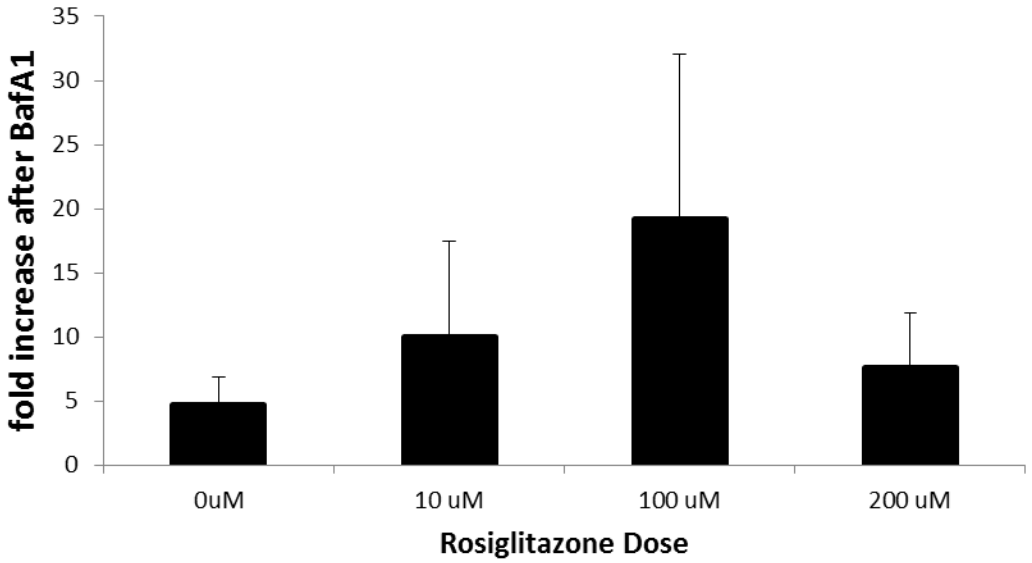

D.

Figure 4-14. Continued C.) Measurement of autophagy as a ratio of LC3II/LC3I in AC16 cells that have been exposed to varying doses of rosiglitazone (n=3). D.) Fold increase after treatment with bafilomycin a1 (Baf/no Baf). Bafilomycin a1 (50nM) is used to assess autophagic flux by inhibiting the formation of the autophagosome to the lysosome, thus preventing degradation.

CHAPTER 5
DISCUSSION

Rosiglitazone was approved by the FDA for administration in the treatment of Type 2 Diabetes mellitus (T2DM) in 1999. With the increase in prescriptions of this medication for T2DM, a concurrent increase in adverse cardiovascular events, such as myocardial infarctions, cardiovascular mortality and cardiac hypertrophy, became apparent. Diabetic patients are already predisposed to heart complications (Vinokur *et al.* 2013), and rosiglitazone clearly exacerbated these symptoms (Starner *et al.* 2008). Because rosiglitazone works by activating the nuclear receptor PPARγ, this study aimed to determine what effects the stimulation of PPARγ by rosiglitazone has on the heart. We hypothesized that 1.) Administration of rosiglitazone will decrease mitochondrial function in the heart, and 2.) Administration of rosiglitazone will increase autophagy in the heart. We tested our hypotheses on cardiac tissue of Fischer 344 rats that had been administered 10mg/kg/day rosiglitazone for 19 days, and cultured cardiomyocytes exposed to varying doses of rosiglitazone. In brief, we found that i.) high doses of rosiglitazone decreased mitochondrial routine respiration and excess capacity in AC16 cells, ii.) mitochondrial enzyme activities (cytochrome c oxidase and citrate synthase) were not affected by rosiglitazone *in vivo* or *in vitro*, iii.) autophagic flux was not affected by rosiglitazone *in vivo* or *in vitro*.

Heart Size is Not Affected by Rosiglitazone Administration

It has been demonstrated that activation of PPARγ by its agonists, like the members of the TZD family, leads to increased expression of the PPARγ receptor (Festuccia *et al.* 2009). Rosiglitazone administration has been shown to induce cardiac hypertrophy (Lee *et al.* 2010). In this particular study, 8 week old mice were

administered 10mg/kg/day rosiglitazone for 4 weeks, and an increase in heart weight to body weight was observed. Lee and colleagues (2010) concluded that the increase in heart size was attributed to an increase in adipose deposition caused by rosiglitazone administration. In addition to increasing adipose deposition, PPARγ agonists stimulate the energy sensing AMPK pathway, which has been shown to induce cardiac hypertrophy in patients with T2DM (Tian *et al.* 2001; Dyck & Lopaschuk, 2006; Festuccia *et al.* 2009).

We hypothesized that administration of rosiglitazone would increase the size of the heart relative to body weight. In this study, Fischer 344 rats were administered 10mg/kg/day for 19 days. In order to determine if this dose and duration of treatment with rosiglitazone had an effect on heart weight, we assessed heart weight normalized to body weight of the Fischer 344 rats after the drug treatment. We determined that 19 days of 10 mg/kg/day rosiglitazone did not have an effect on heart size. We did determine, however, a drug-independent age-related increase in heart weight and normalized heart weight between the young and the middle-aged and old rat, which was likely due to normal heart growth. It is likely that our results do not corroborate with aforementioned studies due to the duration of rosiglitazone administration in our study.

Mitochondrial Enzymes are Not Affected by Rosiglitazone Administration *in vivo*

The activities of the mitochondrial enzymes cytochrome *c* oxidase and citrate synthase are widely used markers of mitochondrial function and content, respectively. Cytochrome *c* oxidase (COX) is one of the electron and proton transporting enzyme complexes (also named Complex IV) of the electron transport system. Citrate synthase (CS) is a component of the Krebs' cycle (citric acid cycle). A commonly applied method to assess COX activity per mitochondrial unit is to normalize the activity of cytochrome *c*

oxidase to that of citrate synthase (Campian *et al.* 2007; Chrzanowska-Lightowlers *et al.* 1993).

We analyzed the activity of these enzymes in cardiac tissue of Fischer 344 rats that had been administered 10 mg/kg/day rosiglitazone or vehicle for a period of 19 days before euthanization. We found that neither age nor treatment, nor an interaction of age and treatment affected CS and COX activity, and COX activity per mitochondrial unit. These findings are corroborated by a 2010 study by Rabol and colleagues on skeletal muscle from diabetic and healthy patients, in which the authors demonstrated that citrate synthase activity and the protein contents of Complexes I-V were not affected by rosiglitazone treatment (4mg/day for 12 weeks). This dose is significantly less than the dose administered to the rats in our study, equating to approximately 0.04mg/kg/day compared to our 10mg/kg/day administration, but the metabolic profiles of the two study organisms also differ greatly in relation to body size. Julie and colleagues (2008) reported that treatment with troglitazone caused mitochondrial dysfunction in livers of patients with Type II Diabetes, although no specific assays of mitochondrial function were performed in this study.

Mitochondrial Enzymes are Not Affected by Rosiglitazone Application *in vitro*

To supplement our *in vivo* work, the activities of cytochrome *c* oxidase and citrate synthase were analyzed in cultured cardiomyocytes (AC16 cells) that were exposed to four concentrations of rosiglitazone (0, 10μM, 100μM, and 200μM) over a four hour period. We found that mitochondrial enzyme activities of COX and CS, representing mitochondrial function and content, respectively, in AC16 cells were not affected by exposure to rosiglitazone regardless of the dose, except in the case of the 10uM rosiglitazone, which decreased COX activity from control. Scatena and colleagues

(2004) reported similar results. The authors found that the activity of cyctochrome *c* oxidase did not differ from control with treatment with ciglitazone, another TZD member (10-50μM for 96hours) in human acute promyelocytic leukemia HL-60 cells.

Interesting to note is that COX activity of AC16 cells significantly decreased from control in the presence of 10μM rosiglitazone. However, when COX activity was normalized to CS activity as indicator of mitochondrial content, the effect dissipated, because CS activity was also lower in those cells, albeit not significantly. These data suggest a decrease in mitochondrial content in this treatment group and preservation of COX function. Removal of depolarized, damaged or dysfunctional mitochondria by autophagy, specifically termed mitophagy, could be the cause for the observed tendency of decreased mitochondrial content after exposure to 10uM rosiglitazone. Further replications of these experiments will have to clarify this connection, because although we determined a numerical increase in autophagic flux in the presence of lower rosiglitazone doses, the difference to control conditions was not significant. .

In addition, this interpretation is contradicted by the association of PPARγ with PGC1α, which is known to induce mitochondrial biogenesis (Huang *et al.* 2011). In support of our speculation, it has been hypothesized that the high doses of TZD's administered for their anti-diabetic effects are acting through a receptor-independent pathway (Festuccia *et al.* 2009). This could mean that the effects we have observed are not caused by a PPARγ-PGC1α interaction, but a result of a receptor-independent effect on the mitochondria (Bolten *et al.* 2007).

High Doses of Rosiglitazone Decreases Mitochondrial Respiration *in vitro*

Normal mitochondrial function is essential for life. It is the driving force behind all biological systems requiring ATP. The heart, especially, relies on proper mitochondrial

function to supply the constant amount of energy needed to perform its function. In the diabetic patient, many subcellular organelles become dysfunctional, including the mitochondria, often leading to cardiomyopathy and heart disease (Xu *et al.* 2012). It has also been reported that TZD's, like rosiglitazone, have been implicated in mitochondrial dysfunction (Brunmair *et al.* 2011; Rabol *et al.* 2010; Julie *et al.* 2008; Sanz *et al.* 2011). We first set out to determine if mitochondrial enzyme activities were affected by rosiglitazone, which we determined were not affected *in vivo* and *in vitro*. We next exposed cultured cardiomyocytes *in vitro* to high (200uM) and low (10uM) doses of rosiglitazone for two different durations, acute (4 hours) and 24 hours and subsequently assessed mitochondrial respiration using High Resolution Respirometry (HRR). Specifically, we measured routine respiration (R), LEAK respiration (L), ETS (E; maximum electron transport capacity), and calculated LEAK control ratio (L/E) and routine control ratio (R/E). We determined that duration of exposure to rosiglitazone did not affect any of these parameters. However, the high dose of rosiglitazone, but not the low dose, caused a decrease of routine respiration and ETS capactity, and both doses had no effect on LEAK respiration. These results demonstrate that rosiglitazone can impair cellular respiration and maximum capacity of electron transport, but that the drug does not affect the "leakiness" of the inner mitochondrial membrane, suggesting that there was not an increase in ROS production. Interestingly, the significant *increase* in routine control ratio (R/E) at the higher rosiglitazone dose reveals that the effect of the drug on maximum capacity is stronger than on routine respiration. The underlying cause for the decreased respiration and maximum capacity of the electron transport chain could lie in damage to one or more of the mitochondrial complexes. We found, however,

that cytochrome *c* oxidase activity, which is Complex IV of the electron transport system, was unaffected by rosiglitazone, and therefore can be eliminated as the limiting factor of the electron transport system. Our respiration experiments were performed on intact cells, and we could not distinguish between activities of individual mitochondrial complexes. Further analysis of mitochondrial respiration in permeabilized cells will be required to determine if other complexes contribute to the observed effects of the drug on cellular respiration.

In a 2010 study, Rabol and colleagues reported that rosiglitazone inhibited Complex I of the electron transport system. A study by Sanz and colleagues (2011) reported that specific activities of Complexes I and III were decreased by 50% and 35%, respectively, by TZD treatment of hepatocytes isolated from Wistar rats after a 30 minute incubation period in 25uM or 100uM rosiglitazone. Hoffman and colleagues (2012) identified an off-target affinity of the glitazones for binding to dehydrogenases like those found in the electron transport system. These findings are corroborated by a 2004 study by Scatena and colleagues that identified a strong inhibitory effect of rosiglitazone on NADH-cytochrome c reductase (combined enzyme activity of complexes I-III). In another study, Pan and colleagues (2006) reported alterations in the inner mitochondrial membrane by rosiglitazone in heart mitochondria of obese compared to non-obese rats. The authors detected changes in the composition of cardiolipin, a phospholipid localized in the inner mitochondrial membrane and essential for optimal function of Complexes I, III, and IV of the electron transport system, (Pan *et al.* 2006). Specifically, they measured an increase in lineolic acid and a decrease in DHA content. DHA is an omega-3 fatty acid, which is known to exert cardioprotective

effects, thus a decrease in DHA content could be pathologically significant (Pan *et al.* 2006). However, it is not known whether altered cardiolipin composition has an effect on mitochondrial complex assembling and function, and maybe the formation of the respiratory supercomplexes (the physical association of all respiratory complexes into a "supercomplex").

Effect of Rosiglitazone on Autophagy in Rat Heart and Cultured Cardiomyocytes

Autophagy is a cellular housekeeping mechanism by which cellular constituents are degraded. Autophagy is activated by several conditions including nutrient or amino acid deprivation, energy imbalance, or activation of the energy sensor AMPK. AMPK leads to an induction of autophagy, which in turn increases the degradation of proteins and thereby replenishes the pool of substrates for energy production. Autophagy has also been shown to be induced by dysfunctional mitochondria, thereby removing these potentially damaging organelles before they can cause further harm (for example by an increased release of free radicals). We hypothesized that treatment with rosiglitazone would induce an increase in autophagic activity, due to 1) its activation of AMPK (Fryer *et al.* 2002), and 2) its negative effect on mitochondrial function, which would induce mitophagy, the autophagic removal of (dysfunctional) mitochondria. We found that autophagy, as indicated by the ratio of LC3-II to LC3-I protein expression, is not significantly affected in rat cardiac tissue after supplementation with 10mg/kg/day rosiglitazone for 19 days, or by age. In general, it has been shown in a variety of tissues and species that autophagy is decreased with age (Cuervo 2009; Yen and Klionsky 2008), but age was not a statistically significant factor in our study. This could be due to to the high variation of protein expression in the rats regardless of age, and the number of animals per group analyzed will have to be increased to draw a definite conclusion.

A reason for the lack of an age-effect could be that the oldest age in our *in vivo* study was 18 months. Fischer 344 rats of that age are not yet considered old, but rather at the transition to senescence, and the decline in autophagic cellular housekeeping might not have commenced.

Similar to rat heart tissue, exposure of AC16 cells to rosiglitazone had no significant effect on autophagic activity. Taken together, we cannot raw clear conclusions based on the results of both our *in vivo* and *in vitro* experiments. More experiments will have to be performed, both *in vivo* and *in vitro*, to increase the power of the analysis. However, if we assume that the numerical increase in autophagic flux (fold increase after BafA1 Figure 4-14D) in AC16 cells in the presence of 10 and 100 uM rosiglitazone compared to controls is a true trend, at least *in vitro*, one could speculate whether this (at this point speculative) increase in autophagy represents an increase in mitophagy, the autophagic removal of (dysfunctional) mitochondria. An increase in mitophagy could be interpreted as a cellular defense mechanism by which further cellular stress caused by damaged, dysfunctional mitochondria is prevented or at least attenuated. The decrease in CS activity (as an indicator of mitochondrial content), albeit non-significant, could suggest increased mitophagy. However, this is speculative and has to be tested with further experiments.

CHAPTER 6
CONCLUSIONS AND IMPLICATIONS

The main finding of our study is that mitochondrial function is impacted by rosiglitazone *in vitro*. In particular, maximum electron transport capacity and routine respiration of AC16 cells were decreased by exposure to high doses of rosiglitazone (200µM), but normalized COX activity was not affected regardless of dose. The precise reason for the observed hindrance of maximum electron transport capacity is not clear in our study, but other groups have speculated on the reason for the negative impact of rosiglitazone on mitochondrial function. For example, Hoffman and colleagues (2012) assessed the off-target binding properties of rosiglitazone, and determined that some of the off-target binding partners of the TZD's are dehydrogenases involved in alteration of mitochondrial respiration, leading to changes in metabolism, energy production and insulin sensitivity. In addition, a 2004 study Scatena and colleagues determined that a 96 hour exposure to ciglitazone induced derangement of the mitochondrial electron system, specifically by inhibiting NADH-cytochrome *c* reductase activity, representing combined activity of Complexes I, II, and III of the electron transport system. And in 2010 Rabol and colleagues reported that rosiglitazone (4mg/day for 12 weeks) affects mitochondrial respiration by inhibiting Complex I of the electron transport system. Interestingly, Pan *et al.* (2006) found that treatment with rosiglitazone caused cardiolipin remodeling in the heart mitochondria of rats, which could impact optimal function of Complexes I, III, and IV of the electron transport system.

In this study, we investigated the effects of rosiglitazone on heart cell bioenergetics by assessing mitochondrial function. The impaired cellular respiration that we detected in the presence of high rosiglitazone concentrations *in vitro* could be an

underlying cause for the adverse cardiovascular effects reported in T2DM patients who received rosiglitazone. The heart depends on sufficient aerobic energy supply. This implies that the heart employs effective energy sensing signaling pathways and tight regulation of substrate supply. The AMP-activated protein kinase (AMPK) is an important master regulator of metabolism (Zaha & Young, 2012), and cellular energy sensor, and it is apparent that the AMPK regulatory pathway is particularly important in the heart. The heart has very little reserved energy and depends on AMPK and proper mitochondrial function to sense energy status and to keep the ATP balance intact (Dyck & Lopaschuk, 2006). Furthermore, activity of AMPK as a master regulator of metabolic has far reaching implications in cellular processes like autophagy and free fatty acid oxidation (Guo *et al.* 2013; Feinstein *et al.* 2005).

AMPK is activated during acute exposure to high concentrations of rosiglitazone (200µM rosiglitazone for 30 minutes) in skeletal muscle cells (Fryer *et al.* 2002; Skrobuk *et al.* 2009;Rabol *et al.* 2010), but whether its stimulation in the diabetic heart is adaptive or maladaptive is unclear. Alterations in AMPK activation have been linked to cardiac hypertrophy, myocardial ischemia and glycogen storage cardiomyopathy (Dolinsky & Dyck, 2006). In hypertrophic cardiac tissues, the AMP:ATP ratio is increased more than 4-fold over control hearts, which would lead to stimulation of AMPK (Tian *et al.* 2001; Dyck & Lopaschuk, 2006). There have been many contradictory reports on the role of AMPK in heart disease (Dolinsky & Dyck, 2006; Fryer *et al.* 2002; Festuccia *et al.* 2009; Dyck & Lopaschuk, 2006). Further clarification of its direct role in cardiac hypertrophy is required to determine if its activation is advantageous or detrimental to cardiovascular health.

AMPK activation has also been linked to upregulation of autophagy (Cerquetti *et al.* 2011). Interestingly, Festuccia and coworkers (2009) have demonstrated that rosiglitazone-induced cardiac hypertrophy was associated with increased turnover of myofibrillar proteins in rats administered 15mg/kg/day for 21 days. The increased turnover was linked to increased protein synthesis, orchestrated by the activation of the mTOR signaling pathway. Similarly to AMPK, the mammalian target of rapamycin, mTOR, is a master regulator of metabolism and anabolic cellular processes. Activation of mTOR stimulates protein synthesis and causes inhibition of catabolic processes, such as autophagy. However, whether the observed activation of mTOR in the hypertrophic hearts was associated with an inhibition of autophagy was not reported. But one could speculate that an inhibition of autophagy would cause the AMP:ATP ratio to shift, causing activation of AMPK, and thereby substantiating the cardiac hypertrophy. Ultimately, we conclude that decreased mitochondrial routine respiration and decreased maximum capacity of the electron transport system is not caused by a decrease in COX IV or CS activity. Further analysis of each individual mitochondrial complex will be required for elucidation into direct site of rosiglitazone action. Others have reported alterations in the composition of the inner mitochondrial membrane caused by TZD treatment, possibly causing a derangement of the supercomplexes. Lastly, our autophagy results were inconclusive. Further replications of the autophagy experiments are required to clarify the role of rosiglitazone on autophagy.

APPENDIX A
CYTOCHROME c OXIDASE ASSAY FOR MICROPLATE READER

Theory

Tissue extract containing cytochrome c oxidase (COX) is added to the test solution containing fully reduced cytochrome c. The rate of cytochrome c oxidation by COX is measured over time as a reduction in absorbance at 550 nm. The reaction is carried out at 30 °C.

Technical note

1. Experience has shown that it is important to use sample homogenates in the same freeze-thaw cycle number. The repeated freezing-thawing seems to enhance COX activity, probably due to further breaking of membranes – but this is just our current working hypothesis. However, it is not clear how often this freeze-thaw cycle could be pursued for maximal activity.
2. Pay attention to footnotes!
3. Check molecular weights (FW) of the chemical and double-check the amount to weigh in for a desired molarity!

Reagents[1]

1. 20 mM KCN (6.512 mg/5 mL dH2O)
2. 100 mM K-Phosphate Buffer
    - make up 0.1 M KH2PO4 (680.45 mg/50 mL dH2O)
    - make up 0.1 M K2HPO4.3H2O (use stock K2HPO4, 870.9 mg/50 mL dH2O)

[1] Check molecular weights (Fw) of the chemical and double-check the amount to weigh in for a desired molarity!

- mix in equal proportions, pH to 7.0

3. 10 mM K-Phosphate Buffer
    - dilute 0.1 M KPO4 Buffer prepared above 1:10 with ddH2O
4. Extraction Buffer (0.1 M KH_2PO_4 Buffer with 2 mM EDTA (29.22 mg/50 mL); pH 7.2)[2]
5. Test Solution
    - Dissolve 50 mg (entire content of horse heart cytochrome c bottle[3]) in 2.5 mL of 10 mM KPO4 buffer
        - Store at -20°C in aliquots (cover tubes with foil)[4]
    - <u>Test solution preparation</u>: (Make daily and wrap in foil)
        - Make up a small volume (1mL) of 10 mg/ml sodium dithionite[5] in 10 mM KPO4 stock solution
            - Needs to be accurate, otherwise reduction won't work correctly; make in a 1.5 ml tube (use <u>within</u> twenty minutes);
        - Add the following reagents in order (see table below). This is important, otherwise reduction won't work correctly.
        - Make enough test solution for the appropriate number of wells (2 wells per sample = duplicates).

[2] Adhihetty *et al.* 2009

[3] Cyt c is the chemical that we run out of most quickly! Pay attention to what we have and order accordingly for your experiment! Sigma C7752-50mg ($94)

[4] The volume of the aliquots depends on the planned runs! Ex.: 50 uL

[5] $Na_2S_2O_4$: Fw 174.11; 10mg/mL = 57 mM

- NOTE: Test solution color should change from dark red/brown to bright pink, indicating cytochrome c was successfully reduced.
- The reduction quality can be assessed, if necessary, by measuring absorbance at 550 and 565 nm. A550/A565 = 10 – 20. If <10, then not reduced enough.

Table A-1. Preparation of test solution.

Test Solution	
(reduced cytochrome c, 2 mg/ml)	23 ml (enough for 82 microplate wells)
Solution of Horse Cytochrome c dissolved in 10 mM KPO4	2.3 ml
10 mg/ml Dithionite in 10 mM KPO4 (make fresh)	92 ul dithionite solution
dH2O	18.4 ml
100mM KPO4	2.3 ml

Procedure

Sample preparation

1. Place powdered[6] muscle samples in liquid N2 storage.
2. Add 50 µl of Extraction Buffer to a 1.5 ml Eppendorf tube per sample on ice. (One tube per sample).
    a. Place tube on scale – Tare – then add sample as described in step #3. Weigh ~ 10 - 20 mg.

[6] The powder-homogenization of the samples can be performed on another day and the samples stored in liq. N2 or -80 °C.

3. Add about 7-10 mg tissue to each tube, recording exact tissue mass. Mix by tapping.
4. Add the volume of Extraction Buffer required to obtain a 20-fold dilution.
    a. Example: 10 mg tissue in 50 µL Extraction Buffer: add 150 µL Extraction Buffer for a total of 200 µL.
5. Mix in thermomixer @ 1400 rmp for 15 min @ Room Temperature (RT).
6. Make up Test Solution during this time and wrap in foil.
7. Following mixing, sonicate each tube 3 x 3 seconds with tube immersed as far as possible in ice-water. Clean the probe between samples with 70% ethanol.[7]
8. Make 80-fold dilution of sample (This is a 1:4 dilution of your 1:20 sample: 70 ul of 20-fold sample + 210 ul of EB = 280 ul total). Keep samples on ice.
9. Centrifuge 80-fold for 2 min at 14,000xg
    a. Collect 80-fold supernatant and keep samples in ice.
10. Collect the supernatant into a new tube and discard the pellet.
11. At this point, set aside 15-20uL of your sample for protein determination using the Bradford Assay. This may also serve as a stopping place, in that case store samples at -80C. Make sure ALL samples have been through the same amount of freeze-thaw cycles.

[7] The desired intensity of sonication for this step of sample prep has nowhere been defined, unfortunately.

Plate reader preparation

12. Open Gen5 plate reader program. Select New Experiment and select *Cytochrome c Oxidase Protocol*. Click the PRE-HEATING setting, enter 30°C and select ON. (Do not run assay until temperature has reached 30°C.) Reading should be in Kinetic mode @ 550 nm.

Reduced cytochrome c preparation

13. Add 270 µl of Test Solution into appropriate number of wells (2 wells per sample for duplicates) of 96-well microplate and incubate in plate reader at 30°C for 10 minutes to stabilize the temperature and absorbance.[8]

14. In Gen5, select Procedure icon, the parameters should be set to a Kinetic Read.
    a. Select Kinetic for Reading Type.
    b. Select Absorbance for Reader and 550 nm for wavelength (drop-down menu).

Proceed with prep and samples

15. Get a second, clean 96 well plate, pipette samples into empty wells (run duplicates of each sample). Recommended volumes: 40 µl of 80-fold extract of muscle tissue

Start of assay

[8] In the plate reader template the reading of the samples is set such that the duplicates are in the same column. Each column will be read separately (see below for more explanation).

16. Remove microplate with Test Solution from the temperature incubator (as long as it has been incubating for 10 minutes @ 30°C). Place this plate beside the plate with the sample extracts in it.

17. Using the multipipette (set to 250 µl) carefully draw up the Test Solution. Make sure the volume is equal in all the pipette tips, and that no significant air bubbles have entered any of the tips.

18. Be sure to double check plate reader settings prior to reading plate.

19. Pipette the Test Solution into the wells with the sample extracts (the second plate). As soon as all the Test Solution has been expelled from the tips (do not wait for the second push from the multipipette), place the plate onto the tray of the plate reader and with the other hand on the mouse, press the OK button. (Speed at this point is paramount, as there is an unavoidable latency period between the time of pressing the OK button and the time of the first reading.)

    a. If running more than 4 samples at a time (4 samples take up 8 wells in the 96-well-microplate for a duplicate measurement of each sample), plate must be read multiple times. It is critical to read the absorbance as soon as reaction has been started. In order to read absorbance as soon as reaction has been started, the reaction must be started (= add test solution to samples) and read (= follow absorbance change for a set amount of time) separately for each column[9] of the plate. That is, add test solution to a column of 8 wells (A though H), read the plate according to the protocol;

[9] columns are numbered 1 through 8; rows are named a through H

at the end the plate comes out and is ready to have next column's reaction started. So, start the reaction in the next column of 8 wells.

20. If desired, add 5 µl KCN (COX inhibitor) to one of the wells to measure any absorbance changes that is independent of COX. This would be your negative control: COX is inhibited and even though the reaction should have been started, the specific catalysis of cytochrome c oxidation won't proceed since the enzyme is inhibited. If there is a absorbance change occurring, it is likely independent of COX activity and therefore unspecific (unless inhibition was unsuccessful; never rule this possibility out!). This activity then needs to be subtracted from the specific activity in your sample.

Preparation of assay program in KC4: this might have to be done above at #10

21. To obtain the rate of change of absorbance over different time periods, select *Options* and enter the amount of time for which you would like a rate of change of absorbance to be calculated. The graph, along with one rate (at whichever time interval is selected) for each sample can be printed on a single sheet of paper, and the results can be saved.

Calculation

COX activity (µmole/min/g tissue) = $\frac{dE^{\text{see footnote}10}/\text{min} \times \text{total volume (ml)} \times 80}{\text{(dilution)}}$

[10] dE/min: absorbance change over time (slope)

18.5 (μmol/ml[11]) x sample vol (ml) x pathlength (cm)[see legend for equation below]

Equation development:

Generic formula for enzyme activity used here:

$$COX\ activity\ [\frac{\frac{\mu mol}{min}}{g\ tissue}] = \frac{dE \times total\ vol \times sample\ dilution}{\varepsilon \times sample\ vol\ \times L}$$

With:

dE: change in absorbance with time [dE/min]; this is the slope of your absorbance-reading curve (linear part)

total vol: total assay volume (here: 290 µL = 0.29 mL)

sample vol: sample volume put into this assay (here: 40 µL = 0.04 mL)

sample dilution: sample prep dilution; in this assay: 80

ε: molar extinction coefficient [SI unit is: $mM^{-1}\ cm^{-1}$; this is the same as: $mol\ L^{-1}\ cm^{-1}$ and $\mu mol\ mL^{-1}\ cm^{-1}$], for cytochrome c: 18.5 $\mu mol\ ml^{-1}\ cm^{-1}$

L: pathlength of the optical path in the spectrophotometer (here: 0.552 cm for plate read in BioTek spectrophotometer plate reader)

Development of the activity unit (µmol/min/g tissue) accordingly:

$$\frac{\mu mol}{\min \times g} = \frac{\mathrm{dE}}{min} \times mL \times 80\frac{mL}{g} \times \frac{1 \times \mu mol \times cm}{18.5 \times mL} \times \frac{1}{mL} \times \frac{1}{0.552\ cm} = \frac{dE \times 80}{18.5 \times 0.552} \times \frac{\mu mol}{min \times g \times}$$

[11] ε: extinction coefficient [$mM^{-1}\ cm^{-1}$ = $mol\ L^{-1}\ cm^{-1}$ = $\mu mol\ mL^{-1}\ cm^{-1}$], (18.5 $\mu mol\ ml^{-1}\ cm^{-1}$)

dE is the slope of the linear part of the absorbance change at the given wavelength that you will obtain from your plate reader's readings over the set period of time. Look at the absorbance change and make sure the linear part is taken. There is the possibility that the later part of the reaction time becomes substrate limiting and the curve levels off.

APPENDIX B
CITRATE SYNTHASE ACTIVITY PROTOCOL

Table B-1. Reaction reagents

Compound name	Final Concentrations	Supplier	Comments
10% Triton X-100	Final Concentration: 0.25%	Promega	10% Triton X-100 stored on shelf
Acetyl CoA	AcCoA Stock: [30 mM] in water Final Concentration in assay: 0.31mM	Sigma (A2181 – 25 mg)	Aliquot in 30 or 25 µL aliquots and store @ -80°C
DTNB	DTNB Stock: [1.01 mM] in 1 M Tris-HCl buffer, pH 8.1; 2mg DTNB + 5mL Tris-HCl Final Concentration in assay: 0.1 mM		Stored in chemical cabinet at RT
Citrate Synthase (positive control)	1:500 dilution in 0.1 M Tris-HCl buffer, pH 7.0	Sigma (C3260)	Positive Control Citrate Synthase (Sigma, C3260); stored @ 4-8°C
Oxaloacetate (make fresh daily)	OAA Stock: [10mM] in 0.1 M triethanolamine-HCL (TEA) buffer pH 8.0; 6.6 mg OAA + 5 mL of 0.1 M TEA buffer Final Concentration in assay: 0.5mM	Sigma (O4126)	OAA powder stored @ -20°C Make 0.1 M TEA buffer dilution fresh before use

[1] Kuznetsov A.V., Lassnig B.-, Gnaiger E. (2010). Laboratory protocol: Citrate synthase. Mitochondrial marker enzyme. *Mitochondrial Physiology Network. 08.14(1-10).*

Procedure

Sample preparation[12]:

NOTE: If running COX activity assay on the same samples, follow the sample preparation instructions in COX protocol and use 80 fold dilution of samples for citrate synthase, skip ahead to protein determination step.

1. Homogenize tissue using BioPulverizer method (see tissue homogenization protocol)
2. Record the weight of tissue added to Cell Lytic MT buffer in 0.6 mL tube (about 5 mg tissue per 100 µl buffer)

[12] Sample prepared for COX activity assay (80 fold dilution) can be used as well

3. Vortex tubes until mixture is homogenous.
4. Centrifuge for 10 minutes @ 12,000 x g and @ 4°C
5. Collect supernatant in a new pre-chilled Eppendorf tube; keep samples on ice.
6. Run a Bradford[13] assay to determine protein concentration of samples.

Protein Determination via Bradford[2] Assay:

1. Prepare BSA protein standards in CelLytic[14] buffer and store in the fridge (4°C).
2. Aliquot about 20 mL of Bradford reagent and let warm up to room temperature.
3. Vortex and pipet 5 µl of each standard and sample, respectively, into separate wells in a 96-well microplate, run triplicates for all standards and samples.
4. Using a multichannel pipet, add 250 µl [15] of Bradford reagent per well.
5. Remove any bubbles using a pin and incubate at room temperature for at least 5 min.

Positive control preparation:

1. Dilute Citrate Synthase enzyme (CS) in a 1:500 dilution using 0.1 M Tris-HCl buffer, pH 7.0;
    a. Add 2 µl CS to 998 µl of Buffer
2. Keep diluted enzyme on ice until activity assay is performed.

Plate reader preparation: (Synergy HT from BioTek; Gen5 operating software)

1. Ensure that program is set to read the appropriate wells on the plate (procedure > plate layout). Set Temp to 30°C.
2. Run kinetic program at 412 nm using the following procedure (Sigma Citrate Synthase Protocol):
    a. Shake: medium intensity for 2 s
    b. READ: 2 min total, 20 s intervals
    c. Plate out/Plate in: Add 10ul of 10mM Oxaloacetate to all wells using multichannel pipet
    d. Shake
    e. READ: 2 min total, 20 second intervals

Start of assay:

1. Based on protein concentration of samples, calculate the amount of sample needed to add 8 µg of protein to each well.

[13] Protein assay: check compatibility of the cell lysis buffer used for sample prep with the assay chemicals. Change assay accordingly, if necessary.

[14] Or in the lysis buffer that was used to prepare the sample!

[15] Use the 300 µl tips for this volume!

Table B-2. Sample preparation per reaction mix

Sample Per Reaction (ug)		8
Sample	Protein Concentration (ug/ul)	Sample Needed (ul)
Horse	3.86	2.1
Cow	2.53	3.2

2. Prepare reaction mixture for each sample and positive control. Follow the scheme shown in the table below. Using the Excel template sheet, enter the amount of sample needed (orange cell); the Excel template will then calculate the amount of each component required for the reaction mix.

Table B-3. Preparation of reaction mix.

Microplate (200 ul)					
Compound Name	Reaction Mix	Reaction Mix + 5 %	Horse Reaction Mix (duplicates)	Cow Reaction Mix (duplicates)	CS Reaction Mix (1:500 & 1:250)
10% Triton X-100	5	5.25	10.5	10.5	10.5
30 mM Acetyl CoA	2.07	2.1735	4.35	4.35	4.35
1.01 mM DTNB	20	21	42	42	42
dH2O	162.93	171.0765	337.8	335.5	340.053
Total	190	199.5	394.6	392.4	396.9
Reaction Mix per Well (ul)		187.9	186.8	189	
Sample (ul)		2.1	3.2	1	
Oxaloacetate (ul)		10	10	10	
Total Reaction (ul)		200	200	200	

The table above shows several different columns:

a) Reaction Mix: every component for correct final concentration without sample, without 5the starter OAA, with only the total amount of water to bring volume to 190 µL; this amounts to the total volume of 190 µL, from which the sample volume needs to be subtracted (from the vol of water), and to which 10 µL of the reaction starter OAA will be added later;

b) Reaction Mix + 5%: it usually is advisable to make a bit more of a bulk reaction mix (Triton, AcCoA, DTNB, water); from this bulk reaction mix, x µL (with x=190-sample vol) will be added to each designated well, and ultimately 10 µL OAA added as starter to reach the total assay volume of 200 µL;

c) Horse Reaction Mix for duplicate measurements: for this everything in the previous column is multiplied by two to provide enough reaction mix for a duplicate run of the same sample. Except the volume of water; for the correct volume of water the sample volume*2 has been subtracted (in the example above: (2*171.0765) – (2*2.1) = 337.9). Same calculations were applied to the cow example and the CS standard/pos control mix. From this sample-specific Reaction Mix 190 minus the sample volume will be pipetted into each

of two wells. Together with sample and 10 uL OAA the volume will add up to 200 uL total reaction volume.

3. Consider the usefulness of preparing a bulk mix of TritonX + AcCoA + DTNB, since those never change volume. A volume of 56.85 µL is needed for a duplicate sample with 5% “safety excess”. Multiply this with the number of samples you plan on running. For individual sample reaction mix preparation take 56.85 µL and combine with the desired volume of water [(2*171.0765) – (2*sample vol)]171.0765*2
4. Once reaction mix is prepared as described, follow the guidelines on the table for pipetting the reaction mix and sample for a total of 190 ul per well.
5. Read plate as described previously. Meanwhile, prepare to add 10 ul of Oxaloacetate per well when instructed to do so (use multichannel pipet). Immediately read plate a second time.
    a. This will follow the following reader protocol @ 30°C.
        1. Run kinetic program at 412 nm using the Citrate Synthase Protocol
        2. Shake: medium intensity for 2 s
        3. READ: 2 min total, 20 s intervals
    ii. The second part of the kinetic reading starts when plate comes out:
        1. Plate out/Plate in: Add 10ul of 10mM Oxaloacetate to all wells using multichannel pipet
        2. Shake
        3. READ: 2 min total, 20 second intervals

Activity Calculation:

1. Use excel sheet to calculate citrate synthase activity using the formula shown in the table below.

Table B-4. Activity calculation of citrate synthase activity

Citrate Synthase Activity					
Sample	ddE [min-1]		dF final	umol/mL/min = IU/mL	umol/min/mg = IU/mg prot
CS 250		0.2134	250	1421.302217	163.3680709
CS 500		0.1101	500	1466.592072	168.5738013
Horse		0.1396	1	3.320621727	0.461197462
Cow		0.1404	1	2.010972692	0.467668068
				0	0
IU/mL	((ddE*Vtot)/(L*13.6*1*Vs))*dF				
IU/mg protein	((ddE*Vtot)/(L*13.6*1*Vs*mg/mL prot))*dF				

LIST OF REFERENCES

Berger, J. P., Akiyama, T. E., & Meinke, P. T. (2005). PPARs: therapeutic targets for metabolic disease. *Trends in pharmacological sciences*, *26*(5), 244–51.

Bolten, C. W., Blanner, P. M., McDonald, W. G., Staten, N. R., Mazzarella, R. a, Arhancet, G. B., Meier, M. F., *et al.*. (2007). Insulin sensitizing pharmacology of thiazolidinediones correlates with mitochondrial gene expression rather than activation of PPAR gamma. *Gene regulation and systems biology*, *1*, 73–82.

Brunmair, B., Staniek, K., Gras, F., Scharf, N., Althaym, A., Clara, R., Roden, M., *et al.*. (2004). Thiazolidinediones, Like Metformin, Inhibit Respiratory Complex I. *Diabetes*, *53*(April), 1052–1059.

Brunmair, B., Staniek, K., Lehner, Z., Dey, D., Bolten, C. W., Stadlbauer, K., Luger, A., *et al.*. (2011). Lipophilicity as a determinant of thiazolidinedione action in vitro: findings from BLX-1002, a novel compound without affinity to PPARs. *American journal of physiology. Cell physiology*, *300*(6), C1386–92.

Campian, J. L., Gao, X., Qian, M., & Eaton, J. W. (2007). Cytochrome C oxidase activity and oxygen tolerance. *The Journal of biological chemistry*, *282*(17), 12430–8.

Cerquetti, L., Sampaoli, C., Amendola, D., Bucci, B., Masuelli, L., Marchese, R., Misiti, S., *et al.*. (2011). Rosiglitazone induces autophagy in H295R and cell cycle deregulation in SW13 adrenocortical cancer cells. *Experimental cell research*, *317*(10), 1397–410.

Chiang, M.-C., Chern, Y., & Huang, R.-N. (2012). PPARgamma rescue of the mitochondrial dysfunction in Huntington's disease. *Neurobiology of disease*, *45*(1), 322–8.

Chrzanowska-Lightowlers, Zosia M. A., Turnbull, Douglass M., and Lightowlers, R. N. (1993). A Microtiter Plate Assay for Cytochrom c Oxidase in Permeablized Whole Cells. *Analytical Biochemistry*, *214*, 45–49.

Cuervo, A. M. (2009). Autophagy and aging: Keeping that old broom working. *Trends in Genetics*, *24*(12), 604–612.

Dolinsky, V. W., & Dyck, J. R. B. (2006). Role of AMP-activated protein kinase in healthy and diseased hearts. *American journal of physiology. Heart and circulatory physiology*, *291*(6), H2557–69.

Dyck, J. R. B., & Lopaschuk, G. D. (2006). AMPK alterations in cardiac physiology and pathology: enemy or ally? *The Journal of physiology*, *574*(Pt 1), 95–112.

Edvardsson, U., Bergstrom, M., Alexandersson, M., Bamberg, K., Ljung, B., and Dahllof, B. (1999). Rosiglitazone (BRL49653), a PPARγ-selective agonist, causes peroxisome-like liver effects in obese mice. *Journal of Lipid Research*, 40: 1177-1184.

Ehrenborg, E. and Krook, A. (2009). Regulation of Skeletal Muscle Physiology and Metabolism by Peroxisome Proliferator-Activated Receptor δ. *Pharmacological Reviews*, 61:373-393.

Feinstein, D. L., Spagnolo, a, Akar, C., Weinberg, G., Murphy, P., Gavrilyuk, V., & Dello Russo, C. (2005). Receptor-independent actions of PPAR thiazolidinedione agonists: is mitochondrial function the key? *Biochemical pharmacology*, *70*(2), 177–88.

Festuccia, W. T., Laplante, M., Brûlé, S., Houde, V. P., Achouba, A., Lachance, D., Pedrosa, M. L., *et al.*. (2009). Rosiglitazone-induced heart remodelling is associated with enhanced turnover of myofibrillar protein and mTOR activation. *Journal of molecular and cellular cardiology*, *47*(1), 85–95.

Fryer, L. G. D., Parbu-Patel, A., & Carling, D. (2002). The Anti-diabetic drugs rosiglitazone and metformin stimulate AMP-activated protein kinase through distinct signaling pathways. *The Journal of biological chemistry*, *277*(28), 25226–32.

Garbern, J. C., Mummery, C. L., & Lee, R. T. (2013). Model systems for cardiovascular regenerative biology. *Cold Spring Harbor perspectives in medicine*, *3*(4).

Garnier, a, Fortin, D., Deloménie, C., Momken, I., Veksler, V., & Ventura-Clapier, R. (2003). Depressed mitochondrial transcription factors and oxidative capacity in rat failing cardiac and skeletal muscles. *The Journal of physiology*, *551*(Pt 2), 491–501.

Gnaiger E (2012) Mitochondrial Pathways and Respiratory Control. An Introduction to OXPHOS Analysis. Mitochondrial Physiology Network 17.18. OROBOROS MiPNet Publications, Innsbruck: 64 pp., 3rd edition.

Hoffmann, B. R., El-Mansy, M. F., Sem, D. S., & Greene, A. S. (2012). Chemical proteomics-based analysis of off-target binding profiles for rosiglitazone and pioglitazone: clues for assessing potential for cardiotoxicity. *Journal of medicinal chemistry*, *55*(19), 8260–71.

Hsiao, G., Chapman, J., Ofrecio, J. M., Wilkes, J., Resnik, J. L., Thapar, D., Subramaniam, S., *et al.*. (2011). Multi-tissue, selective PPARγ modulation of insulin sensitivity and metabolic pathways in obese rats. *American journal of physiology. Endocrinology and metabolism*, *300*(1), E164–74.

Julie, N. L., Julie, I. M., Kende, a I., & Wilson, G. L. (2008). Mitochondrial dysfunction and delayed hepatotoxicity: another lesson from troglitazone. *Diabetologia*, *51*(11), 2108–16.

Kodde, I. F., Van der Stok, J., Smolenski, R. T., & De Jong, J. W. (2007). Metabolic and genetic regulation of cardiac energy substrate preference. *Comparative biochemistry and physiology. Part A, Molecular & integrative physiology*, *146*(1), 26–39.

Koffarnus, R. L., Wargo, K. a, & Phillippe, H. M. (2013). Rivoglitazone: A New Thiazolidinedione for the Treatment of Type 2 Diabetes Mellitus (June). *The Annals of pharmacotherapy*, *47*.

Kuznetsov A.V., Lassnig B. , Gnaiger E. (2010). Laboratory protocol: Citrate synthase. Mitochondrial marker enzyme. *Mitochondrial Physiology Network. 08.14(1-10).*

Lowell, B. B., & Shulman, G. I. (2005). Mitochondrial dysfunction and type 2 diabetes. *Science (New York, N.Y.)*, *307*(5708), 384–7.

Mahmood, D. F. D., Jguirim-Souissi, I., Khadija, E.-H., Blondeau, N., Diderot, V., Amrani, S., Slimane, M.-N., *et al.*. (2011). Peroxisome proliferator-activated receptor gamma induces apoptosis and inhibits autophagy of human monocyte-derived macrophages via induction of cathepsin L: potential role in atherosclerosis. *The Journal of biological chemistry*, *286*(33), 28858–66.

Nissen, S. E., & Wolski, K. (2007). Effect of Rosiglitazone on the Risk of Myocardial Infarction and Death from Cardiovascular Causes. *The New England Journal of Medicine*, *356*(24), 2457–2471.

Nissen, S. E., & Wolski, K. (2010). Rosiglitazone revisited: an updated meta-analysis of risk for myocardial infarction and cardiovascular mortality. *Archives of internal medicine*, *170*(14), 1191–1201.

Pan, H.-J., Lin, Y., Chen, Y. E., Vance, D. E., & Leiter, E. H. (2006). Adverse hepatic and cardiac responses to rosiglitazone in a new mouse model of type 2 diabetes: relation to dysregulated phosphatidylcholine metabolism. *Vascular pharmacology*, *45*(1), 65–71.

Pouwels, K. B., & Van Grootheest, K. (2012). The rosiglitazone decision process at FDA and EMA. What should we learn? *The International journal of risk & safety in medicine*, *24*(2), 73–80.

Rabøl, R., Boushel, R., Almdal, T., Hansen, C. N., Ploug, T., Haugaard, S. B., Prats, C., *et al.*. (2010). Opposite effects of pioglitazone and rosiglitazone on mitochondrial respiration in skeletal muscle of patients with type 2 diabetes. *Diabetes, obesity & metabolism*, *12*(9), 806–14.

Riserus, Ulf, Willett, Walter C., Hu, F. B. (2010). Dietary fats and prevention of type 2 diabetes. *Progressive Lipid Research*, *48*(1), 44–51.

Rubinsztein, D. C., Cuervo, A. M., Ravikumar, B., Sarkar, S., Korolchuk, V., Kaushik, S., & Klionsky, D. J. (2009). In search of an "autophagomometer". *Autophagy*, *5*(5), 585–9.

Scatena, R., Bottoni, P., Martorana, G. E., Ferrari, F., De Sole, P., Rossi, C., & Giardina, B. (2004). Mitochondrial respiratory chain dysfunction, a non-receptor-mediated effect of synthetic PPAR-ligands: biochemical and pharmacological implications. *Biochemical and biophysical research communications*, *319*(3), 967–73.

Smith L. (1955). Spectrophotometric assay of cytochrome c oxidase. *Methods Biochem Anal*, 2; pp. 427–434.

Spiegelman, B. M. (1998). PPAR-y: Adipogenic Regulator and Thiazoidinedione Receptor. *Diabetes*, *47*(3), 507–514.

Spinazzi, M., Casarin, A., Pertegato, V., Salviati, L., & Angelini, C. (2012). Assessment of mitochondrial respiratory chain enzymatic activities on tissues and cultured cells. *Nature protocols*, *7*(6), 1235–46.

Stanley, W. C., Lopaschuk, G. D., & McCormack, J. G. (1997). Regulation of energy substrate metabolism in the diabetic heart. *Cardiovascular research*, *34*(1), 25–33.

Starner, C. I., Schafer, J. a, Heaton, A. H., & Gleason, P. P. (2008). Rosiglitazone and pioglitazone utilization from January 2007 through May 2008 associated with five risk-warning events. *Journal of managed care pharmacy : JMCP*, *14*(6), 523–31.

Tian, R., Musi, N., D'Agostino, J., Hirshman, M. F., & Goodyear, L. J. (2001). Increased Adenosine Monophosphate-Activated Protein Kinase Activity in Rat Hearts With Pressure-Overload Hypertrophy. *Circulation*, *104*(14), 1664–1669.

Troncoso, R., Díaz-Elizondo, J., Espinoza, S. P., Navarro-Marquez, M. F., Oyarzún, A. P., Riquelme, J. a, Garcia-Carvajal, I., *et al.*. (2013). Regulation of cardiac autophagy by insulin-like growth factor 1. *IUBMB life*, (3), 1–9.

Tyagi, S., Gupta, P., Saini, A.S., Kaushal, C., and Sharma, S. (2011). The peroxisome proliferator-activated receptor: A family of nuclear receptors role in various diseases. Journal of Advanced Pharmaceutical Technology & Research. 2011 Oct-Dec; 2(4): 236–240.

Vacek, T. P., Vacek, J. C., Tyagi, N., & Tyagi, S. C. (2012). Autophagy and heart failure: a possible role for homocysteine. *Cell biochemistry and biophysics*, *62*(1), 1–11.

Vinokur V, Berenshtein E, Bulvik B, Grinberg L, Eliashar R, *et al.*. (2013) The Bitter Fate of the Sweet Heart: Impairment of Iron Homeostasis in Diabetic Heart Leads to Failure in Myocardial Protection by Preconditioning. PLoS ONE 8(5): e62948.

Yau, H., Rivera, K., Lomonaco, R., & Cusi, K. (2013). The future of thiazolidinedione therapy in the management of type 2 diabetes mellitus. *Current diabetes reports*, *13*(3), 329–41.

Yen, W.-L., & Klionsky, D. J. (2008). How to live long and prosper: autophagy, mitochondria, and aging. *Physiology (Bethesda, Md.)*, *23*, 248–62.

Zhou, J., Zhang, W., Liang, B., Casimiro, M. C., Whitaker-Menezes, D., Wang, M., Lisanti, M. P., *et al.*. (2009). PPARgamma activation induces autophagy in breast cancer cells. *The international journal of biochemistry & cell biology*, *41*(11), 2334–42.

Zieleniak, A., Wojcik M., and Wozniak, L.A. (2008). Structure and physiological functions of the human peroxisome proliferator-activated receptor γ. *Archivum Immunologiae et Therapiae Experimentalis*, 56: 331-345.

BIOGRAPHICAL SKETCH

Dana Joy Davis Schreffler (born Dana Joy Davis) was born to Frank E. Davis and Christina J. Davis in Phoenixville, Pennsylvania. Dana has a younger brother, Frank E. Davis Jr. In January 1991, her family moved to Palm Coast, Florida where she attended elementary through high school. She graduated from Flagler-Palm Coast High School in May 2005 and in August 2005 she began her undergraduate studies at the Pennsylvania State University Hazelton campus. In 2007, Dana transferred to main Penn State campus in State College, PA, where she participated in undergraduate research in the Langkilde lab. Dana graduated from Penn State in 2009 with a Bachelor of Science in General Biology.

In August 2009, Dana moved to back to Palm Coast, FL where she began work as a laboratory technician in Dr. Dirk Bucher's neuroscience lab at the Whitney Labs of UF working on DNA mapping of the dopamine receptor in *Homarus americanus*. At the Whitney Labs, Dana also performed *in silico* research for the director, Dr. Peter Anderson, collecting an inventory of marine species in the Atlantic Ocean off the east coast of Florida.

In May 2011, Dana began working as a laboratory technician for Dr. Stephanie Wohlgemuth in the Department of Animal Sciences. After working for Dr. Wohlgemuth for a few months, Dana began earning her Master of Science degree as Dr. Wohlgemuth's first graduate student. In March 2012, Dana married Jacob D. Schreffler and changed her name to Dana Joy Davis Schreffler.

In June 2013, Dana successfully defended her thesis entitled, "Effects of the PPARγ agonist Rosiglitazone on Rat Cardiac Tissue and Cultured Cardiomyocytes." Dana intends to pursue a career as a forensic scientist for the state of Pennsylvania.